Transportation of high concentration suspension using visco-plastic lubrication

Saeed Garmeh

A Thesis

In the Department

Of

Mechanical, Industrial and Aerospace Engineering

Montreal, Quebec, Canada

Presented in Partial Fulfillment of the Requirements

For the Degree of

Master of Applied Science (Mechanical Engineering) at

Concordia University

Montreal, Quebec, Canada

CONCORDIA UNIVERSITY

School of Graduate Studies

This is to certify that the thesis prepared

By: Saeed Garmeh

Entitled: Transportation of high concentration suspension using visco-plastic lubrication

And submitted in partial fulfilment of the requirements for the degree of

Master of Applied Science (Mechanical Engineering)

Complies with the regulations of the University and meets the accepted standards with respect to originality and quality.

Signed by the final Examining Committee:

R. Wuthrich Chair

P. Wood-Adams Examiner

C B. Kiyanda Examiner

A. Dolatabadi Thesis Co-Supervisor

I. Karimfazli Thesis Co-Supervisor

Approved by: _____

Chair of Department or Graduate Program Director

_____ 2019 _____ Dean of Faculty

Abstract

Transportation of high concentration suspension using visco-plastic lubrication

Surface engineering plays an important role in different industries. Enhancing the surface properties while keeping the base material properties is the ultimate goal of surface engineering. If the coating is manufactured by melting the particles with heat, it is called thermal spraying. Suspension plasma spraying (SPS) is a branch of thermal spraying where the coating material is suspended in a base liquid. The suspension is injected to a plasma that melts the particles. These molten particles strike the substrate, solidify and form the coating. One of the main challenges in SPS is clogging the suspension in the feeding line. Interaction of the particles with the tube wall may result in sedimentation (fouling) and reduction in the passing area through the tube and finally blockage of the suspension flow. In this case, the spraying process should be stopped and further actions need to be taken for cleaning the suspension line and the injector. The other challenge is the speed of the spraying. SPS is considered as a slow process compared to other conventional thermal spraying methods. Typically, suspensions have concentration of about 10-25 wt. % which means only 10-25 % of the total mass of suspension is made of the particles that actually contribute to the coating. In this study, visco-plastic lubrication is introduced to avoid clogging while increasing the concentration of the suspension up to 70 wt. %. The key element in visco-plastic lubrication is utilizing a yield stress fluid as the lubricant. Yield stress materials behave like fluids if they are submitted to a stress higher than a threshold called yield stress. If the stress is less than that, they behave like solids. In visco-plastic lubrication, a solid protective layer around the core fluid is formed that keeps the core fluid at the center and does not let it touch the tube wall. In this combined experimental and numerical study, the conditions to

establish a stable core-annular flow of suspension-yield stress fluids were determined to transport high concentration suspensions.

Acknowledgement

Hereby I would like to express my sincere thanks to my supervisors, Dr. Ali Dolatabadi and Dr. Ida Karimfazli for their continuous helps and encouragement in this research. This research definitely would not be possible without their dedication and support. Also, I would like to express my thanks to NSERC for financially supporting this study.

Special thanks to my family for their inspirations and emotional supports that always motivates me in life to pursue my dreams. At the end, I am very thankful to Dr. Christian Moreau, Dr. Mohammadreza Attarzadeh, Dr. Mehdi Jadidi, Firoozeh Yeganeh doost, Ali Zabihi, Ali Nozari and Vahid Jalilvand for their helps and technical supports whenever problems encountered.

Outline of the thesis

Chapter one is dedicated to a brief background and origin of lubrication technique and deployment of yield stress material for visco-plastic lubrication.

Chapter two explains the experimental methodology. The setup and the results of the experiments are presented in this chapter.

Chapter three is the simulation and analytical models. The theory of visco-plastic lubrication is explained and the results of the models are presented in this section.

Chapter four is the comparison of the experimental, numerical and analytical models results.

Chapter five explains about the conclusion and future directions of this study.

Table of Contents

List of Figures

List of Tables

List of Symbols

B	Bingham number
L	Tube length
n	Refractive index
R	Tube radius
V_{core}	Core fluid average velocity
V_{lub}	Lubricating fluid average velocity
U_0	Mean axial velocity
ρ_{core}	Core fluid density
ρ_{lub}	Lubricating fluid density
μ_{core}	Core fluid viscosity
μ_{lub}	Lubricating fluid viscosity
τ_y	Yield stress
ΔP	Pressure drop
r_i	Interface radius
Re	Reynolds number
$\dot{\gamma}$	Shear rate

Chapter 1. Introduction and Background

In this chapter. . .

A brief history of annular flows and its application in oil transportation industry will be given. Furthermore, using a yield stress fluid as the lubricant will be discussed.

1.1. Suspension plasma spraying

Suspension plasma spraying (SPS) is a spraying technique where the particles of a desired material are suspended in a base liquid that is called suspension. The Suspension is injected to a plasma that evaporates the base liquid and melts the particles. These molten particles strike the substrate, solidify and form the coating. SPS makes it possible to build a coating from very fine particles. Generally, it is difficult to inject them directly in the form of powder to the plasma due to their low inertia. In SPS, the required momentum is provided by the base liquid. Accelerated particles penetrate the plasma, reaching the hot regions and getting exposed to the required heat for melting.

The feature of using very fine particles helps to build micro and nano structures on a surface that is widely used in manufacturing icephobic and hydrophobic surfaces [1,2], thermal barrier coatings (TBC) and wear resistant coatings for turbine blades. Although SPS has a lot of advantages such as robust control over spraying parameters e.g. power and type of the plasma gas, there are still some challenges associated with this technique. One of the main challenges in SPS is the speed of deposition. SPS is considered as a slow process in comparison to other spraying methods such as cold spray (CS) and high velocity oxy-fuel (HVOF). Typically, Suspensions have concentrations of about 10-25 wt. %. Moreover, the base liquid is evaporated during the spraying and the evaporation absorbs energy from the plasma which is not desirable and results in relatively low efficiency in energy consumption.

The other main challenge is clogging. Interaction of the particles with the tube wall may result in sedimentation (fouling) and reduction in passing area through the tube and finally blockage of the suspension flow. In this case, the spraying process should be stopped and further action need to be taken for cleaning the suspension line and the injector.

In this study, we are looking to come up with a solution for the aforementioned challenges in SPS. The goal is to increase the concentration of the suspensions in SPS while preventing clogging. The ultimate goal is to increase the concentration of the suspension to 70 wt. %. In that case, the spraying process can go much faster with a factor of 3.5 and, since the amount of powder is increased in the unit volume, the base liquid that consumes the energy (undesirably!) is reduced which makes the process energetically optimized.

During SPS, the blockage of suspension flow is quite common, especially when the concentration of solid content is high. Higher concentrations means more interactions between particles and the tube wall. There are two common clogging scenarios. First, when the solid particles in the suspension adhere together and form bigger agglomerates. These agglomerated parts can be trapped in the carrier tube or injector and cause clogging. A visual representation of this phenomena is shown in Figure 1-1.

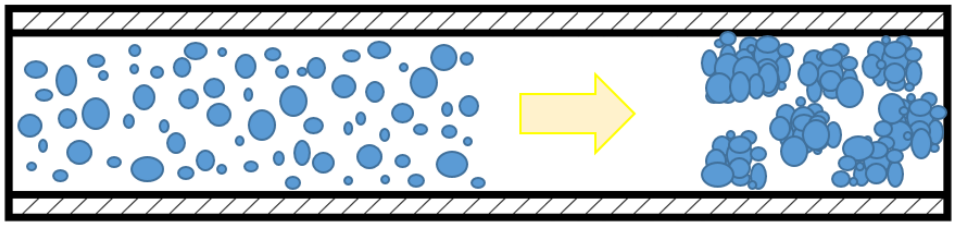

Figure 1-1 Schematic of particle agglemeration during suspension transportation

Second, when these particles interact with the tube wall and injector, they can attach to the tube and decrease the passing area gradually to a point that smaller agglomerates cannot flow through and the flow is suppressed. Figure 1-2 shows this phenomenon schematically.

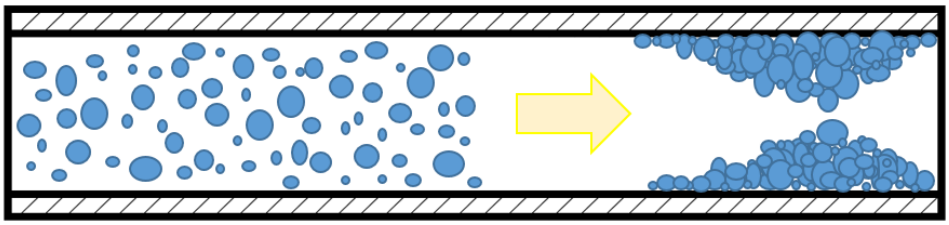

Figure 1-2 Schematic of particle sedimentation

By deploying a technique called visco-plastic lubrication, it is possible to prevent clogging. Visco-plastic lubrication is a subsidery of core annular flows. Core annular flows were popular in transporting heavy oil in the twentieth centurey. The main challenge of heavy oil is its high viscosity that makes the transportation through the pipes difficult demanding extremely high power of pumping [3]. Martínez-Palou et al. [4] investigated general approaches for transportation of crude oil. They studied viscosity reduction by diluting the crude oil and increasing the temperature. There are challenges associated with diluting crude oil like purification of the mixture after transportation [5]. Also, increasing the temperature of oil for reducing the viscosity is not an energy conservative solution.

Establishing core annular flow for reduction in pressure drop was studied by Ghosh et al. [6]. In this technique, water is pumped to oil in a way to form an annular film around the heavy oil. This results in significant reduction of pumping power. They observed that core annular flow can be established for a particular velocity range of core fluid (0.015-0.9 m/s) and lubricating fluid (0.03-1.07 m/s).

1.2. Visco-plastic lubrication

Visco-plastic materials are substances that behave like fluids if they are submitted to a stress higher than a critical value. This critical value is called the yield stress. If the stress is lower than the yield stress, they behave like solids. By using a yield stress fluid as a lubricant, it can be

divided into two regions, yielded and unyielded. In the unyielded part, the stress is below the yield stress. In the yielded part, the stress is higher than the yield stress and the material is considered a fluid. The fluid experiences solid body motion within the unyielded regions.

Frigaard [7] introduced visco-plastic lubrication for annular flows. He studied the stability of a multi-layer plane Poiseuille flow of two Bingham fluids. He showed this kind of flow is more stable than a flow of each of these fluids. He demonstrated visco-plastic lubrication can also be used for transporting a Newtonian fluid in the center of a channel which is lubricated at the walls by a visco-plastic fluid.

Huen et al. [8] demonstrated experimentally that stable core annular flows can be achieved by using a yield stress fluid as the lubricant. They used Xanthan and carbopol as the core fluid and the lubricant respectively. They showed that stable flows can be established by changing the flow rate of the fluids. They acquired different interface diameters by controlling the flow rates.

Mitsoulis [9] discussed the numerical techniques for determining the yielded and unyielded regions in flows of visco-plastic materials such as flows around a sphere and a cylinder and entry and exit flows from dies. He showed progressive growth of the unyielded regions by increasing the Bingham which is dimensionless yield stress.

Hormozi et al. [10] established stable core-annular flow of a viscoelastic core fluid and a yield stress lubricating fluid empirically. They used Carbopol as the lubricating fluid and Polyethylene Oxide (PEO) for the core fluid. They demostrated that an unyielded layer can form around the interface which blocks the growth of instabilities. They showed, at relatively low flow rates of the core fluid, this plug (the unyielded layer surrounding the core fluid) does not break. However, at higher flow rates instabilities are reported. The highest density ratio of core to lubricating fluid for a stable flow they tested was 1.24.

Hormozi et al. [11] modeled the start, development lengths and temporal stability of multilayer flow of a Newtonian core fluid and a Bingham lubricating fluid. They showed the entrance lengths increase with Reynolds number and decrease with Bingham number. They demonstrated for a wide range of parameters, as long as an unyielded plug is formed around the core fluid, interfacial instabilities can be eliminated and a stable core annular flow can be achieved.

Instabilities promoted by density and viscosity difference at the interface of the two fluids can propagate and break the flow configuration [8]. An example of this type of flow is water-lubricated heavy oil. Instabilities appear as waves on the surface of the oil core that arises from density and viscosity difference [12]. In order to stabilize the interface, the interfacial instabilities need to be damped and frozen. The goal of utilizing visco-plastic materials as lubricant for multi-layer flow is to eliminate the instability mechanisms by formation of a plug that covers the core fluid. The geometry of such flows is presented in Figure 1-3. There is a core fluid flowing at the center while lubricated by a yield stress fluid.

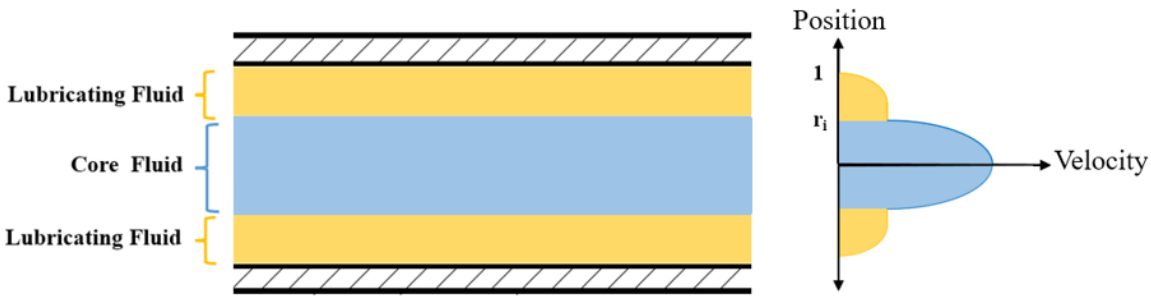

Figure 1-3 Geometry of multilayer flow

In visco-plastic lubrication, there are three types of flow: Stable, Unstable and Static. Generally using yield stress (visco-plastic) materials as lubricant does not guaranty the stability of the flow.

Certain conditions should be met to ensure that the unyielded layer forms. There are three scenarios that can happen while using yield stress material as the lubricant [13].

1.2.1. Stable case

This is the desirable case and the main goal of this work is to establish a stable multilayer flow. This case happens when the lubricant is yielded near the tube wall and unyielded around the core fluid. In other words, a ring of unyielded lubricant is formed around the core fluid. The schematic of the velocity profile is shown in Figure 1-4.

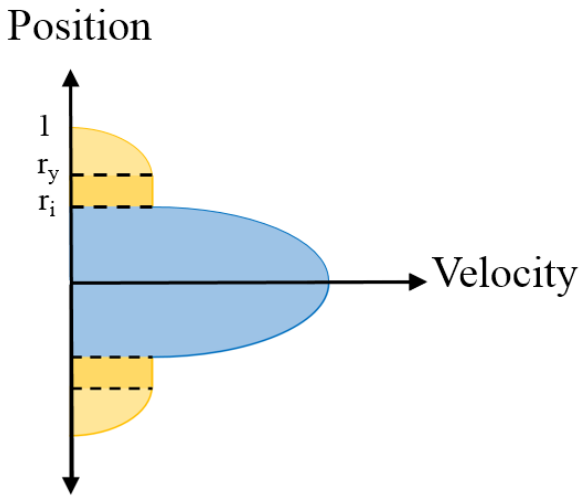

Figure 1-4 Velocity profile for stable case

The radial position is normalized by the radius of the tube, r_y is the normalized yield radius that shows where the stress is equal to the yield stress in the lubricating fluid, and r_i is the normalized interface radius. According to the velocity profile, the unyielded ring is formed with thickness of $(r_y - r_i)$ around the core fluid. In this case, the core fluid can be any suspension and there will be no contact between the suspension and the tube wall.

1.2.2. Unstable case

This is the case where the lubricant is entirely yielded and no plug is formed around the core fluid. Velocity profile is shown in Figure 1-5. This case happens when the yield stress is low and the lubricant yields easily. There is no physical meaning for the yield radius since it lies outside the yield stress fluid [13].

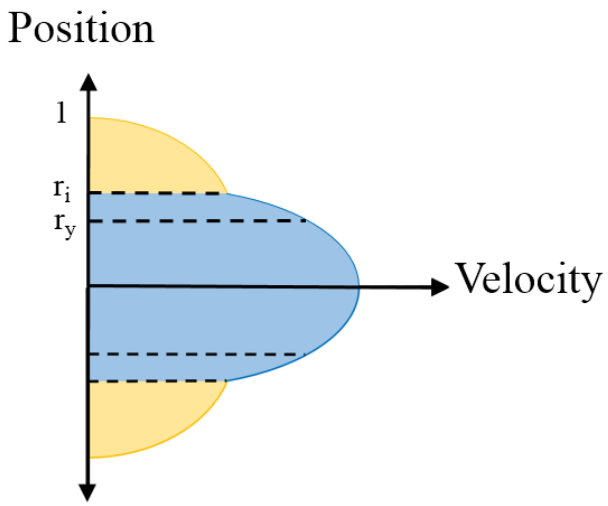

Figure 1-5 Velocity profile for the unstable case

The interface is very sensitive to perturbations. A small instability can propagate if there is no stabilizing mechanism and the mixing starts at the interface. This type of flow is not desirable for us since it cannot form the unyielded layer around the core fluid.

1.2.3. Static case

When the lubricating fluid is entirely unyielded, it cannot move and this means the lubricant is static. Figure 1-6 shows the velocity profile of this flow type schematically. Similar to unstable case, yield radius is located outside the yield stress fluid and that does not have any physical meaning [13]. In static case, the lubricating fluid is fully attached to the tube wall.

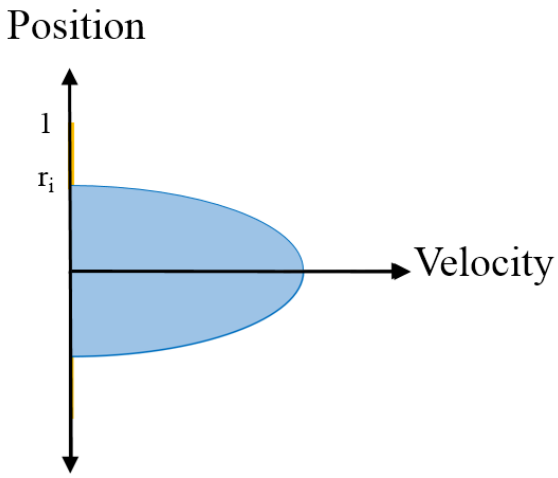

Figure 1-6 Velocity profile for the static lubricating fluid

This flow type is stable. The interface is quite solid and there is no contact of wall and the core fluid. However, this flow type is not desirable. This lubricating layer can act like an imaginary tube with smaller diameter in comparison to the actual tube. This means the agglomeration and sedimentation of particles of the suspension (which is the core fluid) can block the flow over time.

1.3. Objectives

Establishing annular flow for transportation processes brings lots of possibilities and advantages in different frontiers such as prevention of fouling and sedimentation, transportation of viscous fluid and reducing the pressure drop. Using high concentration suspensions in SPS allows to speed up the deposition and coating while lowering the energy consumption. By increasing the concentration, the mass of the base liquid is decreased. Since the base liquid absorbs energy while evaporating, it is expected that the energy consumption will be reduced. It has been reported that at higher concentrations, the chance of agglemoration increases. Visco-plastic lubrication can maintain a stable annular flow where the suspension is enveloped by a plug of the lubricant

material [14] that prevents the contact of the suspension and the tube wall. In that case, high concentration suspensions can be transpoterd without concern about clogging.

The main purpose of this work is to show the feasibility of transportating high concentation suspensions. Furthemore, for enahncing the transportation, the aim is to increase the flow rate ratio of the suspension to the lubricant. In that case, less lubricant will be used which is more desirable.

Chapter 2. Experimental Methodology

In this chapter. . .

The primary factor of the clogging will be introduced. The experimental setup will be explained and the results will be shown.

2.1. Materials and suspension characteristics

Following the goal of this study, transportation of high concentration suspension using visco-plastic lubrication technique, Carbomer gels are used as the lubricating fluid and Titania suspension as the core fluid. Information about these materials and the preparation procedures are discussed in section 2.1.1 and 2.1.2.

2.1.1. Titania Suspension

The suspension that is used in this study is Titanium Dioxide (TiO2) which is also called Titania. Some of the factors that make Titania a reasonable candidate are:

1. Excellent suspendability and suspension's stability

This is an important factor to consider. Since it is desirable to have a suspension with high concentration, it is required to have a stable suspension.

2. Safety and non-hazardous nature of this ceramic powder

In order to reduce the health and safety risks associated with the experiments, the material that is chosen (Titanium Dioxide) is harmless to human beings.

3. Easily obtainable and production in industrial scales

Titania is one of the main white pigments widely used in paints, printing inks, plastics, cosmetics and pharmaceuticals and it is available in the open market.

4. Relative low price

This material is used in the production of hydrophobic surfaces. In this work, water-based suspensions are prepared. Titania suspensions in water are highly stable and are therefore suitable for experiments that need high suspension concentrations. Titania suspensions with

concentrations of 30, 50 and 70 wt. % were prepared and used as the core fluids. The highest concentration of solid content that is investigated in this work is 70 wt. %.

For preparation of Titania suspension, a first beaker is filled with distilled water. It is placed on a magnetic mixer where the rotational speed of the magnet is set to 900 rpm. A sonicator is used to agitate particles in the suspension while adding the Titania powder.

Flow curves of the Titania suspensions are obtained with DHR rheometer. The geometry that is used in the rheology tests is plate-plate and the gap size is set to 500 μm. The device applies different strain rates to the sample and measures the corresponding stress. Flow curves of the suspensions are shown in Figure 2-1.

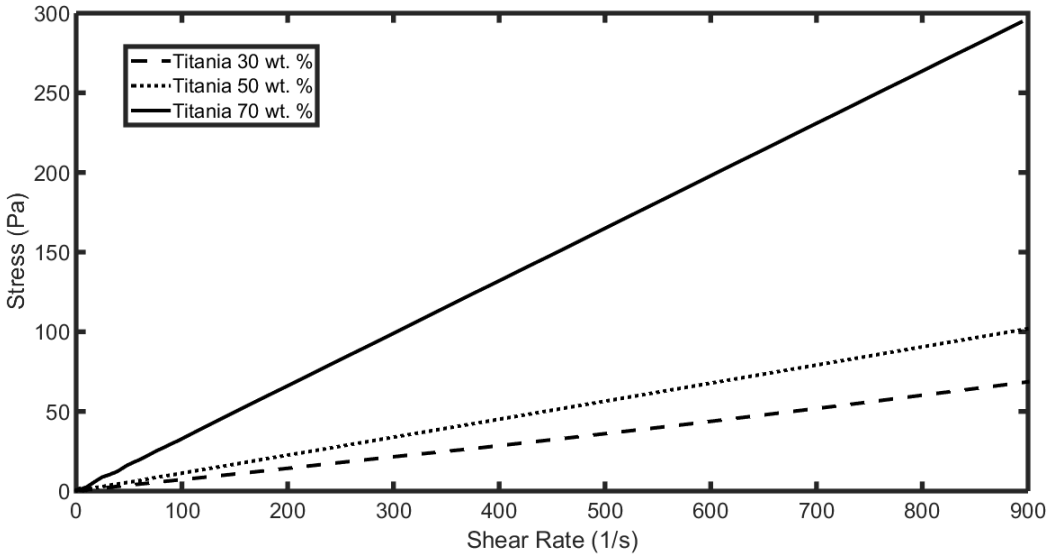

Figure 2-1 Flow curves of Titania suspensions

As depicted in Figure 2-1, the Stress-Strain rate curves for all the suspensions are linear. They all behave like Newtonian fluids. The slopes of the curves are used as their viscosities.

For clarifying the main issue behind clogging, suspensions of Titanium Dioxide (TiO_2) with different concentrations of 30, 50 and 70 wt. % were made and analyzed using a laser diffraction

system (Malvern Spraytec, UK). Measurements presented in Figure 2-2 show no considerable difference. If the suspension is prepared properly, even for high concentrations, there will be no significant change in particle size distribution. Moreover, the agglomeration problem can be solved easily by using chemical methods. The test indicates the main reason behind the clogging is the interaction of particles with the tube wall and the deposition of suspension that was shown in Figure 1-2. This conclusion motivates us to implement a technique for preventing contact of suspension with the tube wall.

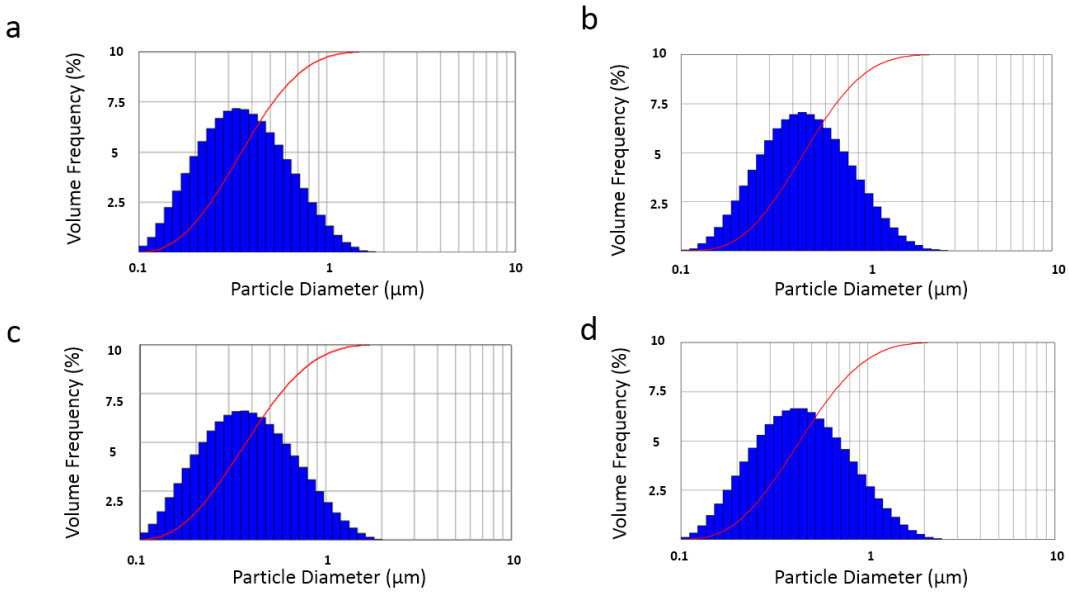

Figure 2-2 Particle size distribution of TiO_2 suspensions with concentrations of (a) 20, (b) 30, (c) 50, and (d) 70 wt. %

2.1.2. Carbomer 940

Carbomer is a water-soluble polymer which is used as viscosity enhancer, gelling and suspending agent in many industries. This material is widely used in manufacturing of cosmetics e.g. gels, creams and lotions, etc. In all the experiments, one concentration of the Carbomer gel is used.

Solutions of Carbomer with concentrations of 0.2 wt. % were prepared. In order to make a homogeneous Carbomer gel, the solution needs to be agitated. After full hydration of the polymer (the raw Carbomer), the solution becomes acidic. To achieve the required yield stress, the solution needs to be neutralized. Therefore, the pH of the solutions is fixed at 6.4 for all the Carbomer gels. Flow curves of the Carbomer gel are presented in Figure 2-3. For yield stress fluids, Herschel-Bulkley and Bingham models are often used for the prediction of flow curves [7,13].

Herschel-Bulkley is a three-parameter rheological model. This model is mathematically described as below:

$$\tau = \tau_y + k\dot{\gamma}^n \qquad \text{Equation (1)}$$

Where τ is the stress, τ_y is the yield stress, $\dot{\gamma}$ is the strain rate, k is the consistency index and n is the flow index. The shear thinning behavior is associated with the $0 < n < 1$ [16]. The Bingham model is a two-parameter rheological model. It includes yield stress and nominal viscosity (or plastic viscosity) of the fluid. The mathematical form of the model is:

$$\tau = \tau_y + \mu_{nom}\dot{\gamma} \qquad \text{Equation (2)}$$

Where τ is the stress, τ_y is the yield stress, μ_{nom} is the nominal viscosity and $\dot{\gamma}$ is the strain rate. By substituting n=1 in the Herschel –Bulkley model, the Bingham model is recovered. By fitting the two models on the experimental data, the corresponding curves for the Carbomer gel are generated. It is important to fit the models on the correct range of strain rate. Fitting the curves over different ranges of shear rates result in different rheology models. $\frac{U_0}{R}$ is used as a measure of the shear rate range. This value gives an approximation of shear rate range for Carbomer gel.

Figure 2-3 shows the experimental data obtained from the rheology measurements and the predicted curves by the two models for Carbomer 0.2 wt. %.

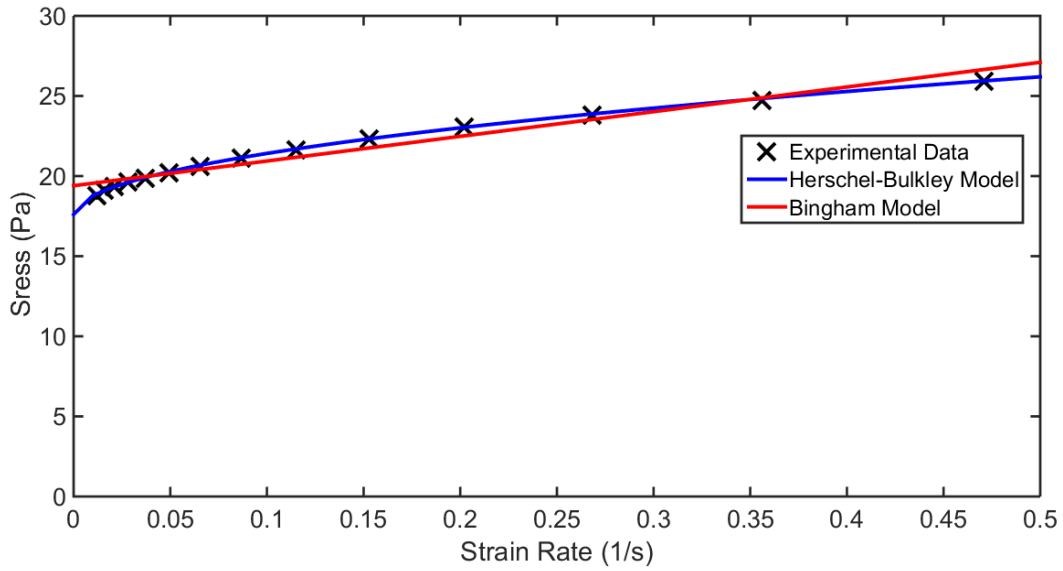

Figure 2-3 Flow curve of Carbomer 0.2 wt. %

As can be understood from Figure 2-3, the Herschel-Bulkley model is more accurate for predicting the behavior of the yield stress fluid [17]. Equations of the curve fits are brought in Table 2-1.

Table 2-1 Predicted curves equations

	Herschel-Bulkley	**Bingham**
Carbomer 0.2%	$\tau = 17.6 + 12.15 \times \dot{\gamma}^{0.5051}$	$\tau = 19.4 + 15.35 \times \dot{\gamma}$

The desirable flow type is a stable case where the core fluid is flowing within an unyielded ring of lubricating fluid. The lubricant is yielded at the wall of the tubes, therefore the unyielded ring of lubricant is moving alongside the yielded part of the lubricating fluid. This flow type has stable

moving interface which makes it unique for our application of transportation. Figure 2-4 shows the schematic of this flow type.

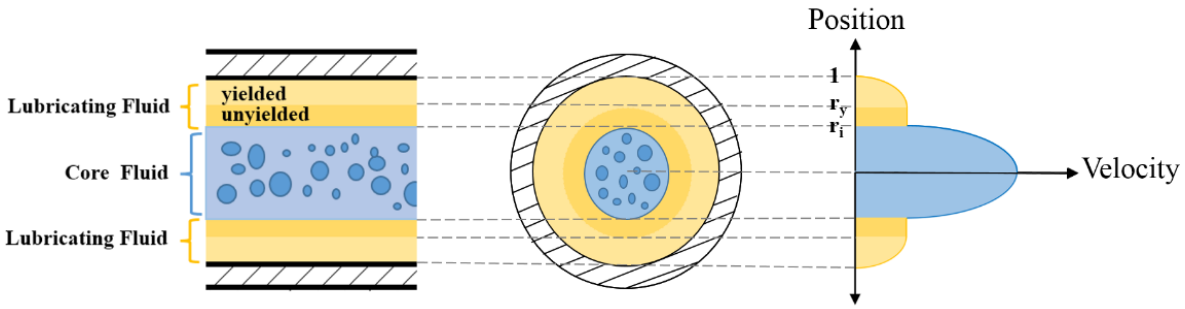

Figure 2-4 Schematic of the stable annular flow

According to Figure 2-4, the layer adjacent to the core fluid is the unyielded portion of the lubricant. The yielded portion is located in the vicinity of the tube wall. The velocity profile shows in the yielded part of lubricant, velocity increases radially from zero at the wall to a definite value at the yield radius. Then, the velocity remains unchanged in the unyielded layer due to its solid-like behavior. This part of the lubricant is responsible for damping and freezing the instabilities arising from the interface. Finally, from the interface of two fluids to the center where the core fluid is flowing, fluid velocity increases and acquires the maximum value at the center.

2.2. Experimental Setup

The primary goal of this work is to demonstrate the possibility of transportation of highly concentrated suspension using visco-plastic lubrication. Three flow types can be established which the desired one is stable annular flow (case 2). Schematic of the test setup is shown in Figure 2-5.

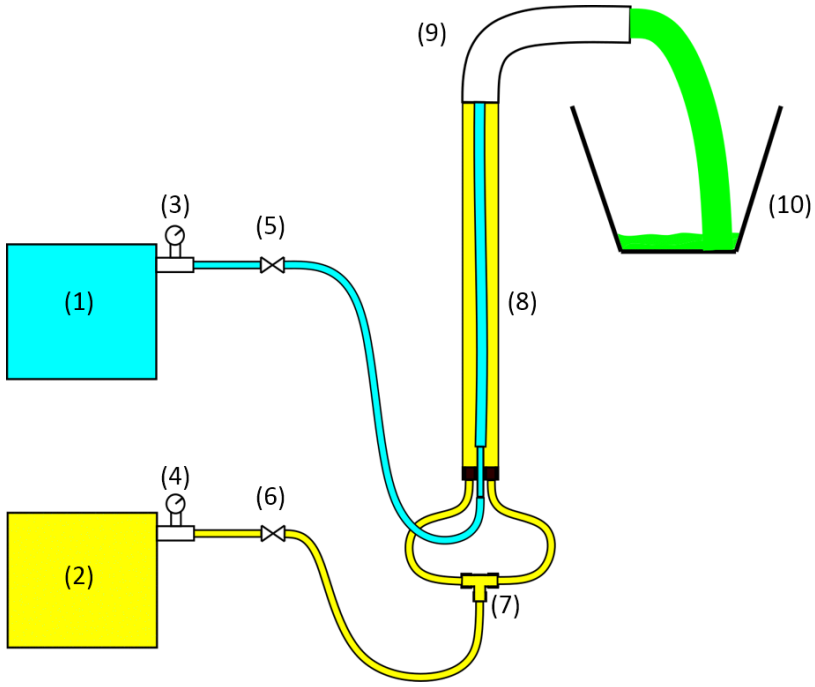

Figure 2-5 Schematic of the experiment setup

Table 2-2 Description of the components

Part Number	Description
1	Pressure tank for core fluid (Titania)
2	Pressure tank for lubricating fluid (Carbomer Gel)
3,4	Pressure regulators
5,6	Control valves
7	Tee connector
8	Plexi-glass tube with ID=38.1 mm
9	Turning
10	Tank for collecting return fluid

As depicted in the schematic, there are two pressure tanks. One contains the core fluid and the other contains lubricating fluid. Pressure vessels are containers which are designed to hold liquids, vapors, or gases at a pressure higher than ambient. In our case, the liquids in the pressure tanks (Carbomer gel and Titania suspension) are pressurized by a gas compressor at 18 psi. This pressure was found to be enough for pumping the Carbomer gel (which is thicker and has yield stress). Pressure gauges connected to the tanks regulate the inside pressure to keep it at a constant value. The flow rates are controlled by two valves.

For uniformly injection of lubricating fluid to the main tube (where the stable annular flow is expected to form), a Tee Connector is used in the path to divide the flow of lubricating fluid into two branches. These branches finally connect to the bottom of the main tube for generating peripheral flow of lubricating fluid.

The core fluid (which is Titania suspension) is connected to an injector placed at the center of the main tube. The suspension is expected to flow at the center while lubricated by the lubricating fluid. The tubes that connect the pressure tanks to the main tube are 3/8” in diameter. The injector has an inner diameter of 1/4" and an outer diameter of 1/2”.

At the end of the tube, there is a 90-degree turning. The diameter of this turning is equal to the outer diameter of Plexi-glass tube and it leads the flow to an open tank. The tank, which is placed at the end of the flow path, will gather the mixture of the two fluid (Titania suspension and Carbomer gel).

In the experiments, the average volumetric flow rates are calculated by dividing the mass of the fluid pumped by the density by the time. The mass of each fluid that is pumped is measured by

weighing the fluids in the tanks and the open container before and after the experiment. Using the density correlation, and the time, the average flow rate can be calculated.

The Plexi-glass tube has an inner diameter of 1 1/2"and an outer diameter of 1 3/4" which is sealed at its two ends. An image of the actual setup is shown in Figure 2-6.

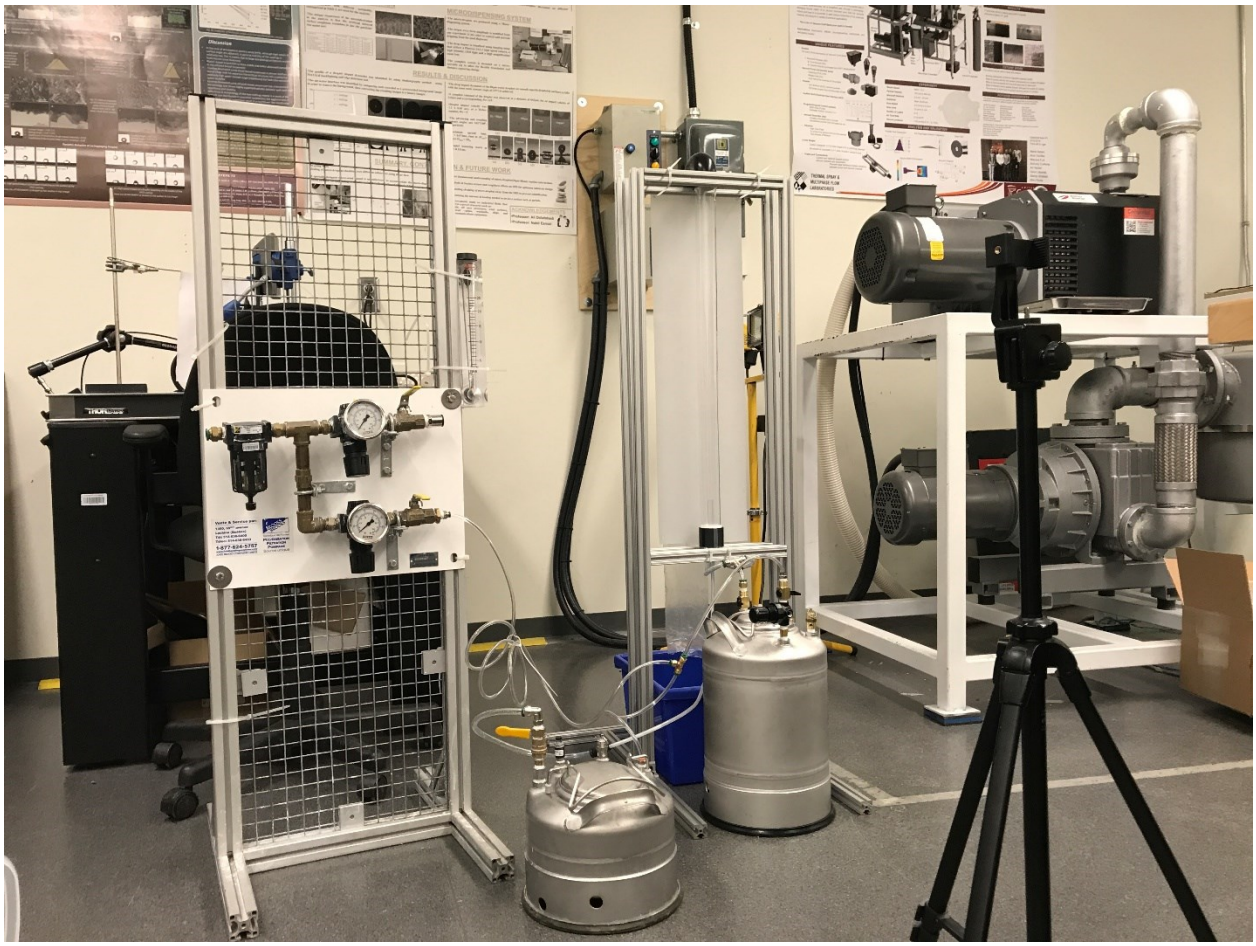

Figure 2-6 Experimental setup

For establishing the annular flow, first the tube needs to be filled with the Carbomer gel. After the tube is filled with the Carbomer gel, the suspension is injected. In the experiments, there is control over the flow rates of the fluids by the control valves and changing the pressure of the pressure tanks. After the flow starts and it reaches steady state conditions, an image of the multi-

layer flow inside the main tube is taken for interface detection. Then it is processed and the average interface radius is calculated. Snapshots of the flow are presented in Figures 2-7 and 2-8.

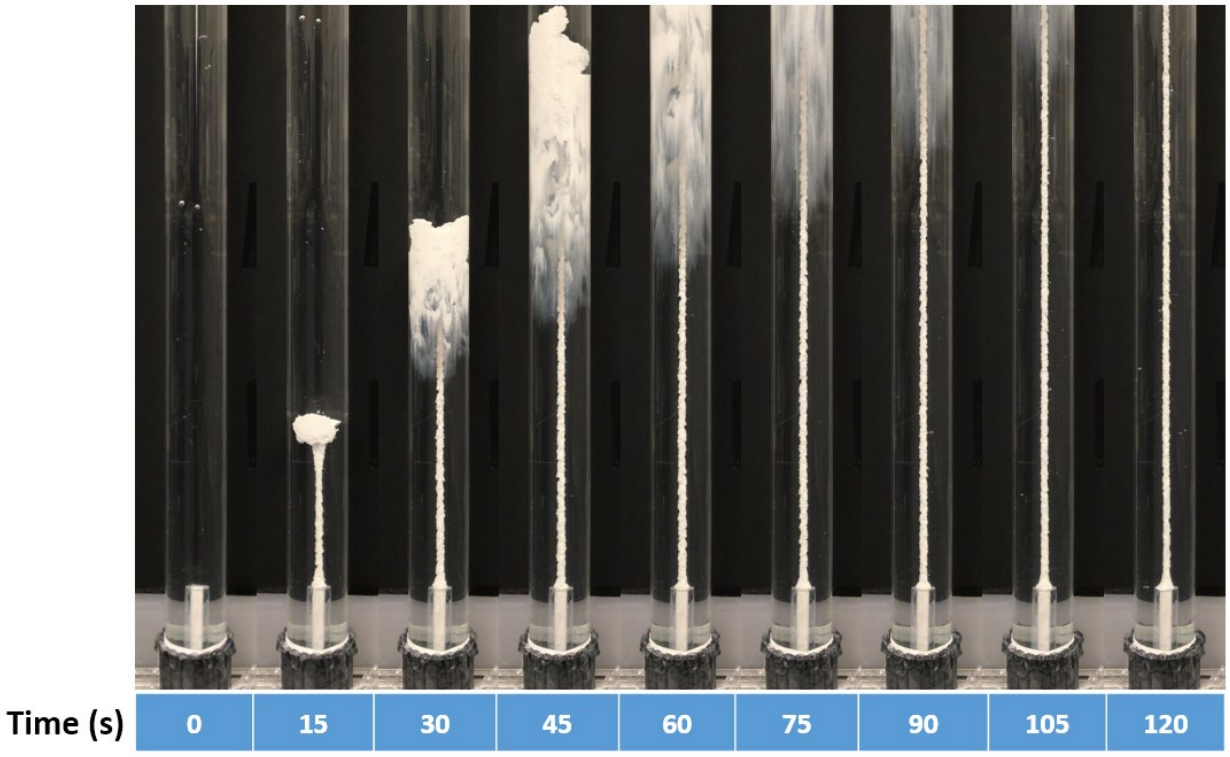

Figure 2-7 Illustration of the flow evolution for Titania suspension (core fluid) and Carbomer gel (Lubricant)

Figure 2-7 shows the flow of Titania suspension that is lubricated by Carbomer gel. As it is shown, at the startup of the flow, a cloud (white color) forms and the two fluids are mixed together. As the flow develops, a clear interface that forms near the injector and there is no sign of the cloud inside the tube. These images cover 60 cm of the tube length. Similar to Figure 2-7, Figure 2-8 shows more forms of the cloud and development of a clear and sharp interface.

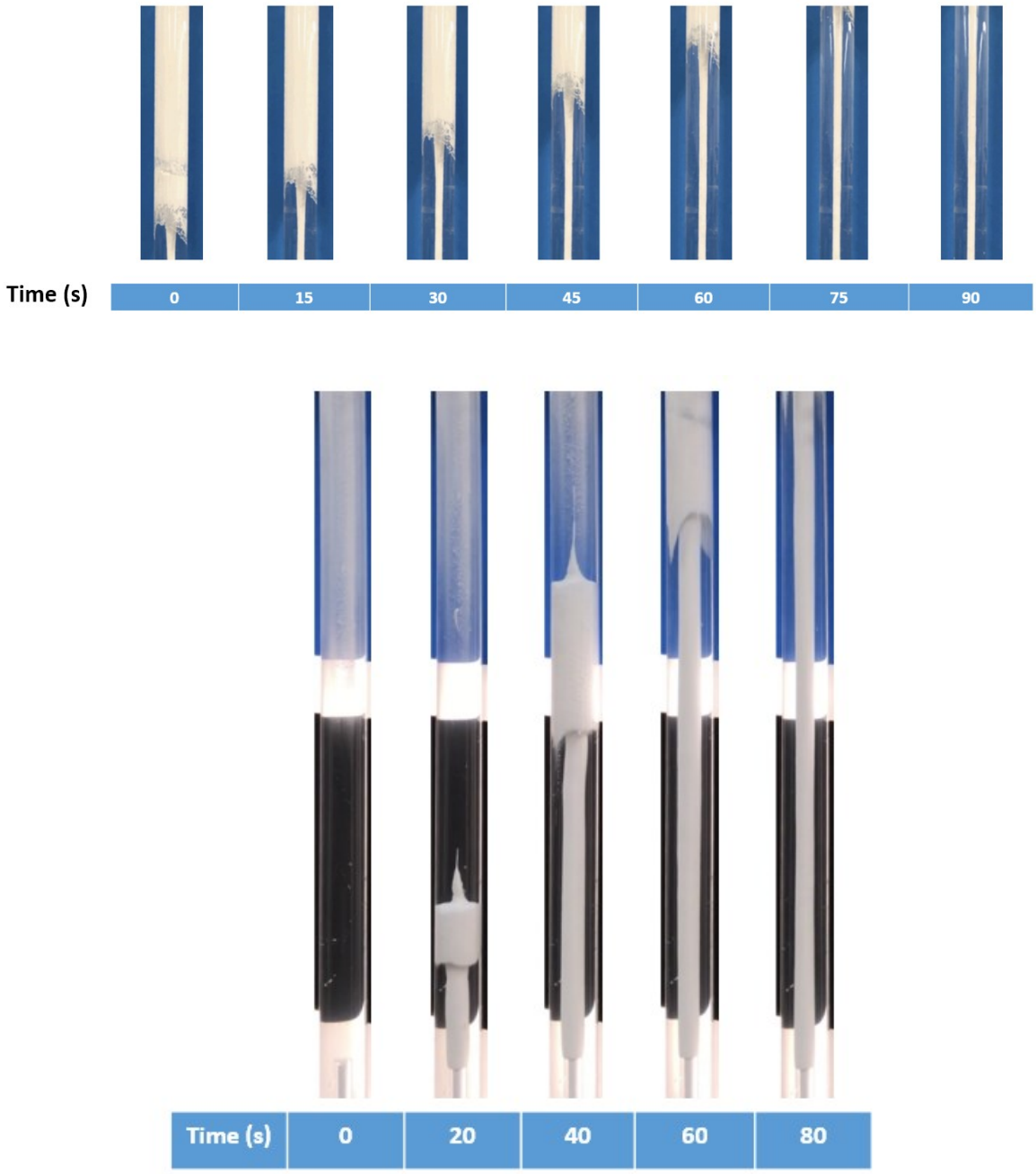

Figure 2-8 Snapshots of the flow of the Titania suspension (white color) and the Carbomer gel

2.3. Experiment Results

2.3.1. Proof of concept

As introduced before, the goal and the novelty of this work is to transport the suspension. For the first step, Titania 30 wt. % was used as the core fluid. By using Carbomer 0.2 %, the stable annular flow of Titania 30 wt. % suspension and Carbomer 0.2% gel is established. Below, you can see the snapshot of the steady part of the flow in the middle of the tube far from the injector and the exit.

Figure 2-9 Steady flow of Titania 30 wt. % lubricated by Carbomer 0.2% gel, Q_{core}=7.7 mL/s and Q_{lub}=4.6 mL/s

By acquiring the desirable flow type which is denoted as the stable case, it is proved that the concentration of suspension can be increased and the clogging issue will be postponed. For the next steps, the concentration of Titania suspensions is increased. Increasing the concentration is promising since the ultimate goal is to use visco-plastic lubrication in SPS and speed up the process. Therefore, experiments were performed to find the limit for the suspension concentrations.

2.3.2. Effect of suspension concentration

Results of the experiments are presented into 3 steps. For all the experiments, Carbomer gel with concentration of 0.2 wt.% is used. That is to say the rheology of the lubricant is constant. By increasing the concentration of Titania suspension, the aim is to establish stable annular flow. Now we focus on the interface diameter which is measured from the experiments. Then we compare it with the interface diameter predicted by the numerical and analytical models. The average of the interface diameter is calculated and corrected by a MATLAB code which takes fisheye effect into account. It is described in section 2.4 with more details.

2.3.2.1. Titania 30 wt. % suspension

For this step, Titania 30 wt. % suspension is used as the core fluid and Carbomer 0.2 wt. % as the lubricant. In all the experiments, the flow is in upward direction (against the gravity). Density of Titania 30 wt. % is 1.32 g/mL. The snapshots that are presented in these sections are covering 80 mm of the middle length of the tube.

Figure 2-9 shows that instabilities at the interface are frozen in the unyielded portion of the Carbomer gel. In other words, interfacial perturbations are frozen in the plug around the core fluid and there is no mixing or formation of a cloud. More details about the experiments in this step are provided in Table 2-3.

Table 2-3 Experiments with Titania 30 wt.% suspension

	Core fluid flow rate (mL/s)	**Lubricating fluid flow rate (mL/s)**	**Flow rate ratio (Q_{core}/Q_{lub})**	**Interface diameter (mm)**
Experiment 1	7.7	4.6	1.67	5.7
Experiment 2	9.5	5.8	1.64	7.1
Experiment 3	10.3	4.0	2.57	8.7
Titania 30 wt. % density= 1.32 g/mL				

2.3.2.2. Part 2: Titania 50 wt.% suspension

In this step, Titania 50 wt. % suspension is used as the core fluid. Lubricating fluid is Carbomer 0.2 wt. %. The density of Titania 50 wt. % is 1.55 g/mL. Figure 2-10 shows a snapshot of the steady flow for one of the experiments in this section.

Figure 2-10 Steady flow of Titania 50 wt. % lubricated by Carbomer 0.2% gel, Q_{core}=5.2 mL/s and Q_{lub}=4.3 mL/s

Details of the experiments are presented in Table 2-4.

Table 2-4 Experiments with Titania 50 wt.% suspension

	Core fluid flow rate (mL/s)	**Lubricating fluid flow rate (mL/s)**	**Flow rate ratio (Q_{core}/Q_{lub})**	**Interface diameter (mm)**
Experiment 1	4.2	3.8	1.55	5.6
Experiment 2	5.2	4.3	1.67	5.8
Experiment 3	9.3	4.8	1.93	7.1
Titania 50 wt. % density= 1.55 g/mL				

2.3.2.3. Part 3: Titania 70 wt. % suspension

In this section, the concentration of Titania suspension is increased to 70 wt. %. It means the suspension has 70% solid content (Titania powder). The same lubricant (Carbomer 0.2 wt. %) is used in this section. Density of the suspension is measured to be 2.20 g/mL. A snapshot of the steady state flow for one of the experiments is presented in Figure 2-11.

Figure 2-11 Steady flow of Titania 70 wt. % suspension and Carbomer 0.2% gel, Q_{core}=5.8 mL/s and Q_{lub}=2.4 mL/s

More details about this part can be found in Table 2-5.

Table 2-5 Experiments with Titania 70 wt.% suspension

	Core fluid flow rate (mL/s)	**Lubricating fluid flow rate (mL/s)**	**Flow rate ratio (Q_{core}/Q_{lub})**	**Interface diameter (mm)**
Experiment 1	5.2	4.0	1.29	9.4
Experiment 2	5.8	2.4	2.41	12.5
Titania 70 wt. % density= 2.20 g/mL				

2.4. Fisheye effect and light refraction

For measuring the interface radius, the "Fisheye effect" needs to be considered. The light beams emitted from the interface of the two fluids travel in a circular tube and get refracted as the environment changes. As a result, the interface of the two fluids appears larger on the recorded image than its actual size. Therefore, a correlation between the interface diameter that the observer sees and the actual diameter need to be devised. Figure 2-12 shows the journey of the light beams from its origin to the observer.

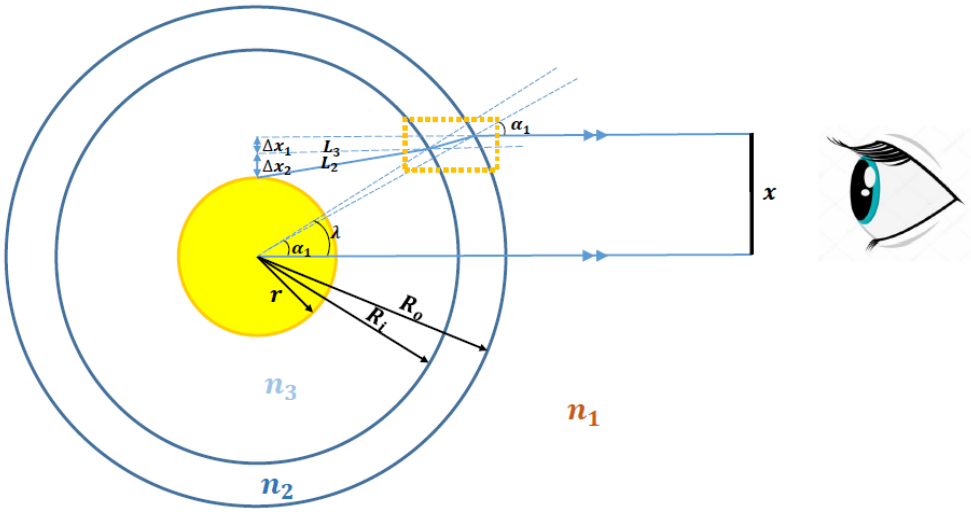

Figure 2-12 Fisheye effect

In Figure 2-12, r is the radius of the interface, R_i is the inner radius of the tube, R_o is the outer radius and x is the radius that is seen by the observer. According to Figure 2-12, the light beam travels in the Carbomer gel, then it reaches the tube wall. After refraction, it comes to the observer's eye. Angles and refractions of the light are shown in Figure 2-13 with more details.

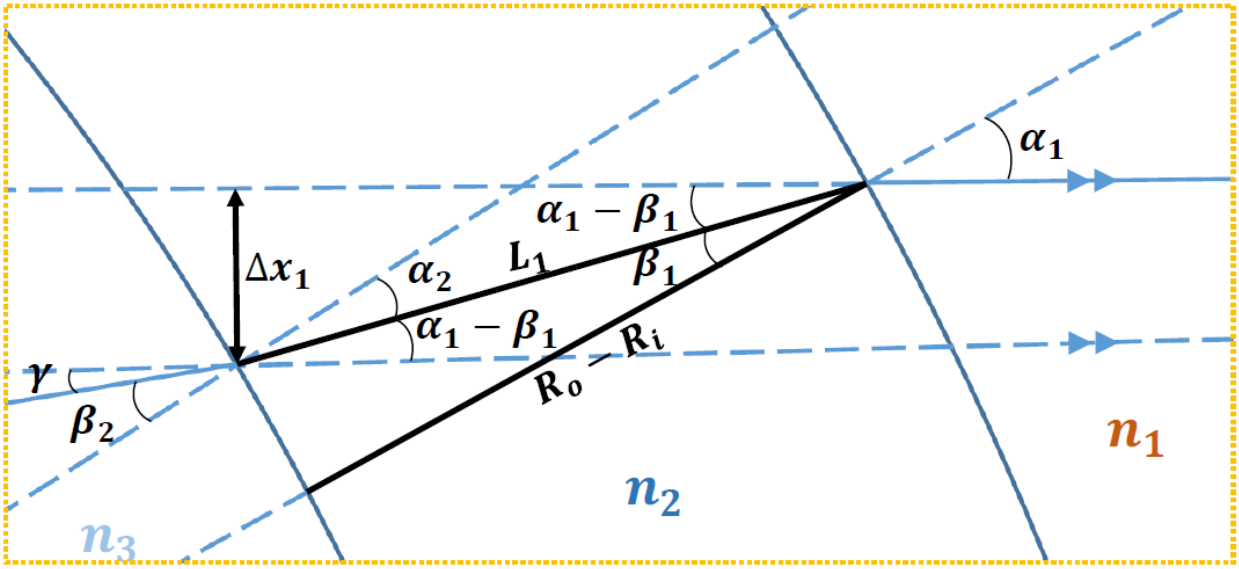

Figure 2-13 Refraction of the light through the tube wall

The refractive index of water is used for the Carbomer gel inside the tube (n_3). The tube wall is Plexiglas (n_2) and the environment is air (n_1). Refraction equations are listed below:

$$\sin\alpha_1 = \frac{x}{R_0} \qquad \text{Equation (3)}$$

$$\alpha_1 = sin^{-1}\left(\frac{x}{R_0}\right) \qquad \text{Equation (4)}$$

$$n_1 sin\alpha_1 = n_2 sin\beta_1 \qquad \text{Equation (5)}$$

$$\beta_1 = sin^{-1}\left(\frac{n_1 sin\alpha_1}{n_2}\right) \qquad \text{Equation (6)}$$

$$cos\,\beta_1 \approx \frac{R_o - R_i}{L_1} \qquad \text{Equation (7)}$$

$$L_1 = \frac{R_o - R_i}{cos\,\beta_1} \qquad \text{Equation (8)}$$

$$\Delta x_1 = L_1 \sin\left(\alpha_1 - \beta_1\right) \quad \text{Equation (9)}$$

$$sin\lambda = \frac{x - \Delta x_1}{R_i} \quad \text{Equation (10)}$$

$$\lambda = \sin^{-1}\left(\frac{x - \Delta x_1}{R_i}\right) \quad \text{Equation (11)}$$

$$n_2 sin\alpha_2 = n_3 sin\beta_2 \quad \text{Equation (12)}$$

$$\beta_2 = sin^{-1}\left(\frac{n_2 sin\alpha_2}{n_3}\right) \quad \text{Equation (13)}$$

$$\gamma + \beta_2 = \alpha_2 + \left(\alpha_1 - \beta_1\right) \quad \text{Equation (14)}$$

$$\gamma = \alpha_2 + \left(\alpha_1 - \beta_1\right) - \beta_2 \quad \text{Equation (15)}$$

$$L_3 = R_i \cos\left(\beta_2 + \gamma\right) \quad \text{Equation (16)}$$

$$L_2 = \frac{L_3}{\cos\gamma} \quad \text{Equation (17)}$$

$$\Delta x_2 = L_2 sin\gamma \quad \text{Equation (18)}$$

$$r = x - \Delta x_1 - \Delta x_2 \quad \text{Equation (19)}$$

To ensure the integrity of the above correlations, an object with known diameter was placed inside the tube (filled with the Carbomer gel for mimicking the experiment conditions) and the measured diameter using the above correlations was in a good agreement with the actual diameter of the objects with less than 2 percent difference. If the interface is noncentric, the error could be

larger which is not accounted in the correlations. Because of the uncertainty associated with the assumption of centric core fluid, the 2 percent error can be neglected.

2.5. Edge detection

In order to measure the interface radius of the two fluids, the images taken during the experiments are analyzed. Resolution of the images is 0.1 mm/pixel that provides good accuracy for edge detection. Using MATLAB edge detector, the raw images were analyzed and the average interface diameter was calculated. An example of the detected edges are presented in Figure 2-14. The interface diameter is calculated by averaging the distance of the two edges. The interface diameter is 9.4 mm after correction due to the Fish-eye effect.

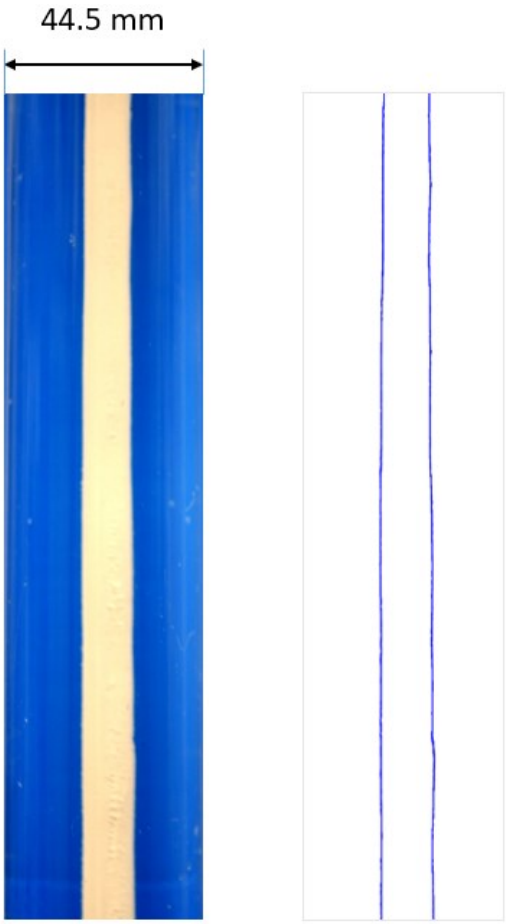

Figure 2-14 A snapshot of the flow and the detected edges

Chapter 3. Numerical and Analytical Models

3.1. Numerical Modelling

In this part, the problem is studied using numerical modelling. ANSYS Fluent is used for simulation of the flow. Laminar solver and Mixture model are used for simulation of the multiphase flow of the two fluids. Mixture model is capable of calculating non-Newtonian viscosity [18]. Continuity and Momentum equations are solved based on the mixture properties. Mixture density and mixture velocity are computed based on the volume fraction of each phase. Herschel-Bulkley and Newtonian models are used for the viscosity of the lubricating and core fluids, respectively.

3.1.1. Governing Equations

3.1.1.1. Continuity Equation

$$\frac{\partial(\rho_m)}{\partial t} + \nabla.(\rho_m \vec{v}_m) = \upsilon \qquad \text{Equation (20)}$$

Where ρ_m is the mixture density according to Equation (21) and $\vec{v}_m$ is the mass-averaged velocity according to Equation (22):

$$\rho_m = \sum_{k=1}^{n} \alpha_k \rho_k \qquad \text{Equation (21)}$$

$$\vec{v}_m = \frac{\sum^{n} \alpha_k \rho_k \vec{v}_k}{\rho_m} \qquad \text{Equation (22)}$$

Where *n* is the number of phases. Current numerical study is for a flow of two phases. α_k , ρ_k and $\vec{v}_k$ are volume fraction, density and velocity of phase *k*, respectively. *k*=1 is representing the lubricating fluid and *k*=2 is the core fluid.

3.1.1.2. Momentum Equation

$$\frac{\partial}{\partial t}(\rho_m \vec{v}_m) + \nabla \cdot (\rho_m \vec{v}_m \vec{v}_m) = -\nabla p + \nabla \cdot (\mu_m (\nabla \vec{v}_m)) + \rho_m \vec{g} \qquad \text{Equation (23)}$$

Where μ_m is the viscosity of the mixture:

$$\mu_m = \sum_{k=1}^{n} \alpha_k \mu_k \qquad \text{Equation (24)}$$

3.1.1.3. Volume Fraction Equation for the Secondary Phase

From the continuity equation for secondary phase (k=2), the volume fraction equation for secondary phase 2 can be obtained:

$$\frac{\partial}{\partial t}(\alpha_2 \rho_2) + \nabla \cdot (\alpha_2 \rho_2 \vec{v}_m) = 0 \qquad \text{Equation (25)}$$

3.1.2. Geometry and computational domain

The computational domain is a cylinder with diameter of *D* and length of *L*. The grid is made of 211,167 quadrilateral cells that are generated by ICEM CFD. A grid dependency study is done for ensuring the results are independent from the mesh. Figure 3-1 shows the domain and the grid used in this study. The mesh is sufficiently refined in order to capture the velocity gradient in layers next to the tube wall. Figure 3-2 shows the velocity profile of the annular flow with three different mesh resolutions. It indicates the studied mesh has less than 1 % error from the very fine one.

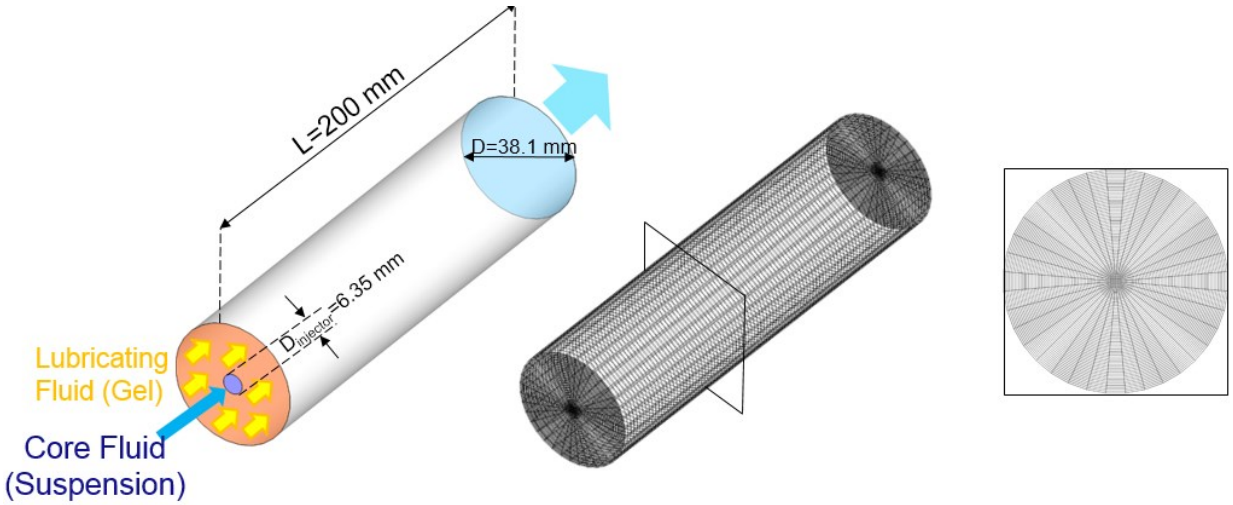

Figure 3-1 Domain, grid and resolution of the mesh

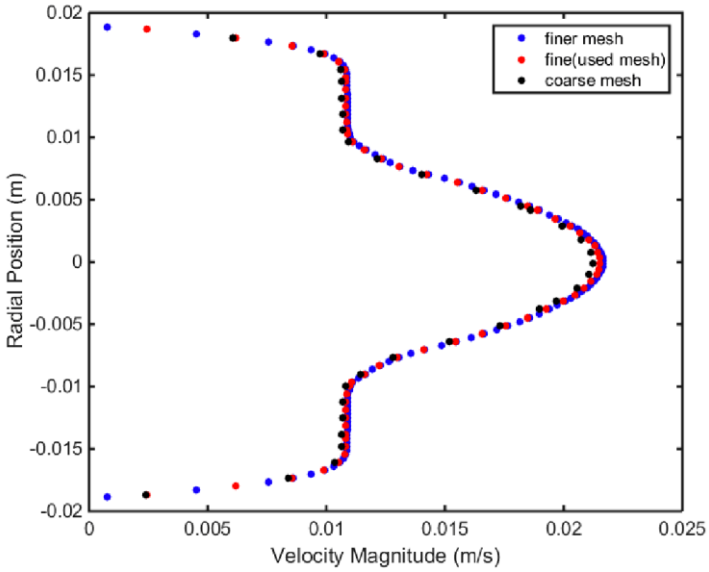

Figure 3-2 Velocity profile for different mesh resolutions

3.1.3. Boundary conditions

Velocity inlet boundary condition is assigned for the inlets of the core and lubricating fluids. The core fluid is injected at the center of the cylinder while the lubricating fluid is injected peripherally. Pressure outlet used as the boundary condition at the exit of the domain and the wall boundary condition with no-slip is assigned to the tube wall. Properties of the fluids are set based on the results of the rheology tests.

3.1.4. Dimensional Analysis

Table 3-1 shows a list of parameters that contribute to our visco-plastic lubrication problem.

Table 3-1 Parameters

	Name	sign
Average velocity	Core fluid	V_{core}
	Lubricating fluid	V_{lub}
	Mean axial velocity	U_0
Density	Core fluid	ρ_{core}
	Lubricating fluid	ρ_{lub}
Viscosity	Core fluid	μ_{core}
	Lubricating fluid	μ_{lub}
Tube	Length	L
	Radius	R
Yield stress	Lubricating fluid	τ_y
Pressure drop		ΔP
Injector radius		r

According to The Buckingham Pi theorem, groups of dimensionless numbers are as presented in Table 3-2.

Table 3-2 Dimensionless groups

$\Pi_1 = \frac{\rho_{core} V_{core} r_i}{\mu_{core}}$	$\Pi_2 = \frac{\tau_y R}{U_0 \mu_{lub}}$	$\Pi_3 = \frac{\Delta P}{\rho_{core} V_{core}^2}$	$\Pi_4 = \frac{\mu_{core}}{\mu_{lub}}$
$\Pi_5 = \frac{V_{core}}{V_{lub}}$ or $\frac{Q_{core}}{Q_{lub}}$	$\Pi_6 = \frac{\rho_{core}}{\rho_{lub}}$	$\Pi_7 = \frac{L}{R}$	$\Pi_8 = \frac{r}{R}$

According to Table 3-2, Π_1 is the Reynolds number (*Re*) which is the ratio of inertial forces to viscous force, where the Reynolds number is calculated based on the property of the core fluid, Π_2 is the Bingham number (B) which is the ratio of yield stress to viscous stress for the lubricating fluid, Π_3 is dimensionless pressure drop; Π_4 is viscosity ratio of core fluid to lubricant which is denoted by *m*;

Π_5 is the ratio of average velocity of core fluid to lubricating fluid. The flow rate ratio is easier to control experimentally, therefore, the flow rate ratio is used instead of average velocity ratio. Π_6, Π_7 and Π_8 are the ratios of two (homogenous) parameters for normalization.

Among the introduced dimensionless numbers, the principal ones are Reynolds, Bingham and viscosity ratio [11]. By changing the parameters of those dimensionless groups, the stable annular flow can be established.

3.2. Numerical Results

For each experiment introduced before, a simulation based on the obtained data is performed. Measured flow rates in the experiments and the rheologies of the fluids are used as inputs. As an illustration, the color map of volume fraction of core fluid and velocity magnitude obtained from the simulations is presented in Figure 3-3. Along the tube, the core fluid expands and shortly it becomes fully developed. The interface in the simulation is defined by the volume fraction of 0.5

(after the flow fully developed) and the core fluid velocity reaches 0.15 m/s near the centerline. Large portion of the lubricating fluid moves with velocities less than 0.025 m/s (or 25 mm/s) that shows how slower is the movement of lubricant in compare to the core fluid. Interface diameters for each simulation are presented in Table 3-3.

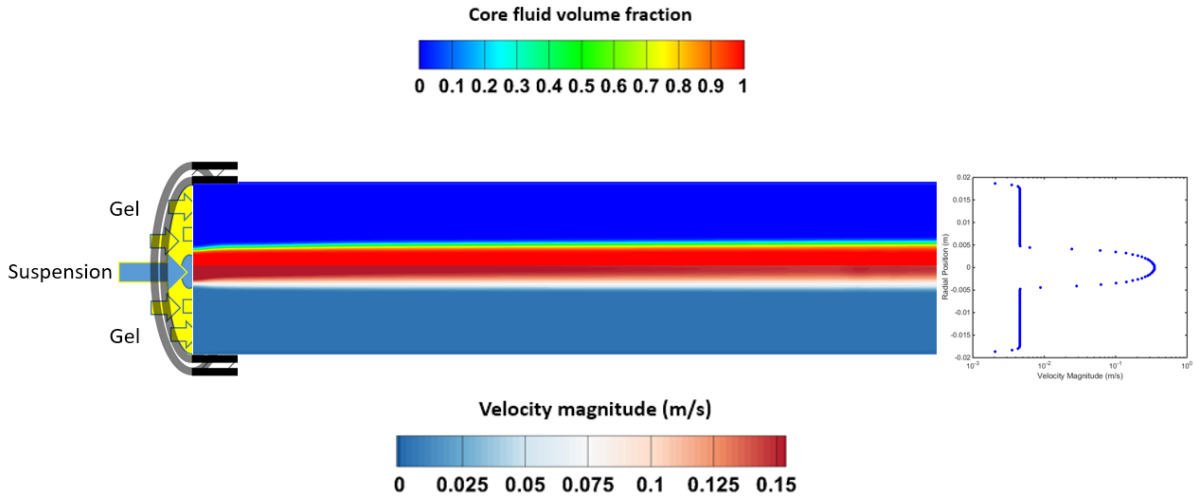

Figure 3-3 Color map of core fluid volume fraction and velocity magnitude for Titania 50 wt.%

Table 3-3 Interface Diameter Predicted by the Numerical Model (mm)

	Simulation 1	**Simulation 2**	**Simulation 3**
Titania 30 wt. %	6.2	7	6.5
Titania 50 wt. %	8.4	6.8	7.2
Titania 70 wt. %	10.3	12.9	-

In the simulations, Herschel-Bulkley model is used for the lubricating fluid. Herschel-Bulkley model is more precise and accurate for predicting the behavior of the yield stress fluid since it

fits well the rheology data compared to the Bingham model which is used in the analytical model. It considers the shear thinning behavior of the lubricating fluid and according to the Figure 2-3, the predicted curve by Herschel-Bulkley model fits well enough the data points obtained from the experiment.

Based to the simulations, all the cases were found to be stable similar to what is observed in the experiments. To understand what would happen for even higher concentrations, numerical modelling can be of great help. Nine simulation cases were modelled where the viscosities and flow rates of the core fluids are changed. Lubricating fluid properties and flow rates kept constant. According to the data obtained from rheology, by increasing the core fluid concentration, It is expected that the viscosity increases. Therefore, the viscosity of the core fluid is increased for a hypothetical suspension with concentration higher than 70 wt. %. To optimize the transportation process, we tend to increase the flow rate ratio of core fluid to lubricating fluid. Figure 3-4 shows the velocity profiles of the simulation cases. Lubricating flu id is the same Carbomer gel 0.2 %. However, the viscosity of the core fluid is increased to represent a higher concentration suspension.

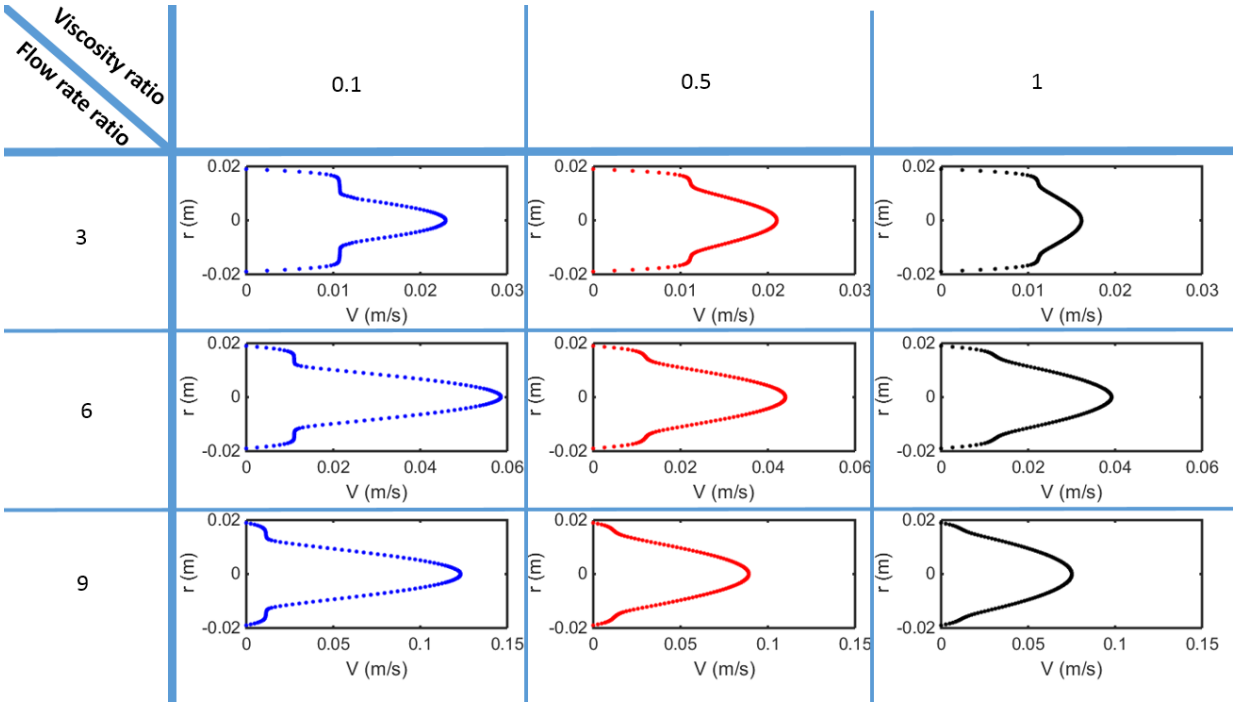

Figure 3-4 Velocity profile of simulation cases for different flow rate ratios and viscosity ratios

For having the desirable flow, an unyielded plug should be formed around the core fluid. This unyielded region acts like a wall and the velocity is constant throughout this region. According to Figure 3-4, for the viscosity ratio of 0.1 (which is 5 times larger than the viscosity ratio of Titania 70 wt.% to the lubricant), there are stable flows for the three flow rate ratios (of core to lubricating fluid) due to the formation of an unyielded plug. The thickness of the plug is reduced by increasing the flow rate ratio which is also desirable. By increasing the viscosity ratio to 0.5, no unyielded plug is formed and all the cases are considered as unstable. Still, increasing the viscosity ratio to 1 results in no unyielded region around the core fluid and for the three flow rate ratios, the flows are found to be unstable. In all the simulation cases, the interface radius is found to increase with viscosity ratio and flow rate ratio.

3.3. Theoretical Analysis

3.3.1. Flow classification

Following Moyers-Gonzalez et al. [13], the flow is stable if :

$$m < \frac{-3Br_i^4}{Br_i^4 + 3B - 4Br_i - 12r_i} \qquad \text{Equation (26)}$$

$$m > \frac{Br_i^4}{4} \qquad \text{Equation (27)}$$

Where m is the viscosity ratio of core fluid to lubricating fluid, B is the Bingham number. r_i is the interface radius that is normalized by the tube radius (R). If the inequality signs are replaced by equality, the equations will show the borders between stable-unstable-static cases.

Therefore,

$$m = \frac{-3Br_i^4}{Br_i^4 + 3B - 4Br_i - 12r_i} \qquad \text{Equation (28)}$$

$$m = \frac{Br_i^4}{4} \qquad \text{Equation (29)}$$

Equation (28) shows the border between stable and unstable cases and Equation (29) shows the border between stable and static cases.

By plotting the equations (1) and (2) for a specific Bingham number, say $B=2.5$ (Which is the average of Bingham numbers in the experiments), there will be three flow regions, namely *Stable*, *Unstable* and *Static*.

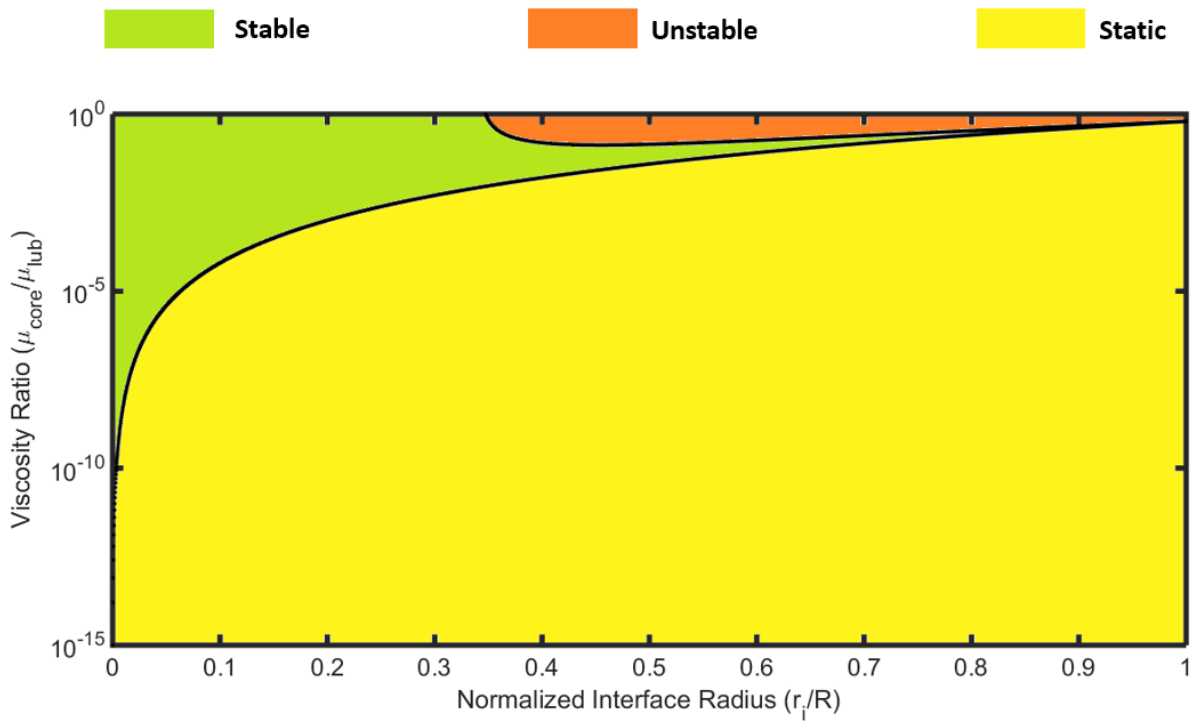

Figure 3-5 plot of viscosity ratio vs. normalized interface radius for *B=2.5*

The green region shows when the flow is stable. The unyielded layer of lubricating fluid is formed which covers the core fluid. As discussed before, this is the region of interest! Yellow regions correspond to static case where the lubricant is remained fully unyielded and it is stuck to the tube wall. There will be no movement of the peripheral fluid. Orange region is showing unstable case where the lubricant is fully yielded and a small perturbation at the interface results in the mixing of the core fluid and lubricating fluid. This is the region to avoid!

3.3.2. Flow rate ratio

Following Moyers-Gonzalez et al. (2004), velocity profile for the stable case is:

$$V(r)=\begin{cases}\dfrac{B}{2r_y}\left[\dfrac{1}{m}(r_i^2-r^2)+(1-r_y)^2\right] & 0\le r\le r_i \\ \dfrac{B}{2r_y}(1-r_y)^2 & r_i\le r\le r_y \\ \dfrac{B}{2r_y}\left[(1-r_y)^2-(r-r_y)^2\right] & r_i< r\le 1\end{cases} \qquad \text{Equation (30)}$$

The yield radius is determined by solving the following equation:

$$0=r_y^{\,4}-4r_y\left(1+\frac{3}{B}\right)+3\left(1+\frac{r_i^4}{m}\right) \qquad \text{Equation (31)}$$

In this equation, velocity is normalized by the mean axial velocity of the flow $\frac{Q_t}{A}$ where Q_t is the total flowrate of Q_{core} + Q_{lub} and A is the cross section of the tube.

For determining the flow rate ratio, the flow rate of core fluid is needed to be divided by the flow rate of the lubricating fluid. Considering that:

$$Flow\ Rate\ Ratio=\frac{Q_{core}}{Q_{\text{lub}}}=\frac{\int_0^{r_i}\frac{B}{2r_y}\left[\frac{1}{m}(r_i^2-r^2)+(1-r_y)^2\right]2\pi r dr}{\int_{r_i}^{r_y}\frac{B}{2r_y}\left[(1-r_y)^2\right]2\pi r dr+\int_{r_y}^{1}\frac{B}{2r_y}\left[(1-r_y)^2-(r-r_y)^2\right]2\pi r dr} \qquad \text{Equation (32)}$$

Flow rate ratio of the two fluid is:

$$\frac{Q_{core}}{Q_{\text{lub}}}=\frac{\frac{r_i^2(1-r_y)^2}{2}+\frac{r_i^4}{4m}}{\frac{(1-r_y)^2(r_y^2-r_i^2)}{2}+\frac{(1-r_y)^3(5r_y+3)}{12}} \qquad \text{Equation (33)}$$

For unstable case, velocity profile is as follows:

$$V(r)=\begin{cases}\dfrac{B}{2r_y}\left[\dfrac{1}{m}(r_i^2-r^2)+(1-r_y)^2-(r_i-r_y)^2\right] & 0\le r\le r_i\\ \dfrac{B}{2r_y}\left[(1-r_y)^2-(r-r_y)^2\right] & r_i<r\le 1\end{cases} \qquad \text{Equation (34)}$$

And yield radius is calculated by solving the following equation:

$$0=r_y(4r_i^3-4-\frac{12}{B})+3(1+\frac{r_i^4}{m}-r_i^4) \qquad \text{Equation (35)}$$

Flow rates and flow rate ratio by following the same approach would be:

$$Flow\ Rate\ Ratio=\frac{Q_{core}}{Q_{\text{lub}}}=\frac{\int_0^{r_i}\frac{B}{2r_y}\left[\frac{1}{m}(r_i^2-r^2)+(1-r_y)^2-(r_i-r_y)^2\right]2\pi r dr}{\int_{r_i}^{1}\frac{B}{2r_y}\left[(1-r_y)^2-(r-r_y)^2\right]2\pi r dr} \qquad \text{Equation (36)}$$

$$\frac{Q_{core}}{Q_{\text{lub}}}=\frac{\frac{(1-2m)r_i^4}{4m}-(1-r_i)r_i^2r_y+\frac{r_i^2}{2}}{\frac{(1-r_i)^2(3(1+r_i)^2-4(1+2r_i)r_y)}{12}} \qquad \text{Equation (37)}$$

Velocity profile for static case is as follows:

$$V(r)=\begin{cases}\dfrac{B}{2r_y}\left[\dfrac{1}{m}(r_i^2-r^2)\right] & 0\le r\le r_i\\ 0 & r_i<r\le 1\end{cases} \qquad \text{Equation (38)}$$

As it can be understood from the velocity profile, from interface towards the tube wall, velocity is 0 which shows the lubricating fluid is static and stuck to the wall.

Yield radius is determined by the equation below:

$$0=4r_y m-Br_i^4 \qquad \text{Equation (39)}$$

Flow rate ratio for the static case is:

$$Flow\ Rate\ Ratio = \frac{Q_{core}}{Q_{\text{lub}}} = \frac{\int_0^{r_i} \frac{B}{2r_y}\left[\frac{1}{m}(r_i^2 - r^2)\right] 2\pi r dr}{\int_{r_i}^{1} [0] 2\pi r dr} = \infty \qquad \text{Equation (40)}$$

In this case, since the lubricating fluid is static, the flow rate of lubricant will be zero and this implies the flow rate ratio of core fluid to lubricating fluid is infinity. It is worth mentioning that in unstable and static cases, the physical meaning of r_y is not as a yield surface, since r_y lies outside the Bingham fluid domain [13].

By plotting the flow rate ratio for each region against the normalized interface radius for $B=2.5$, Figure 3-6 will be generated.

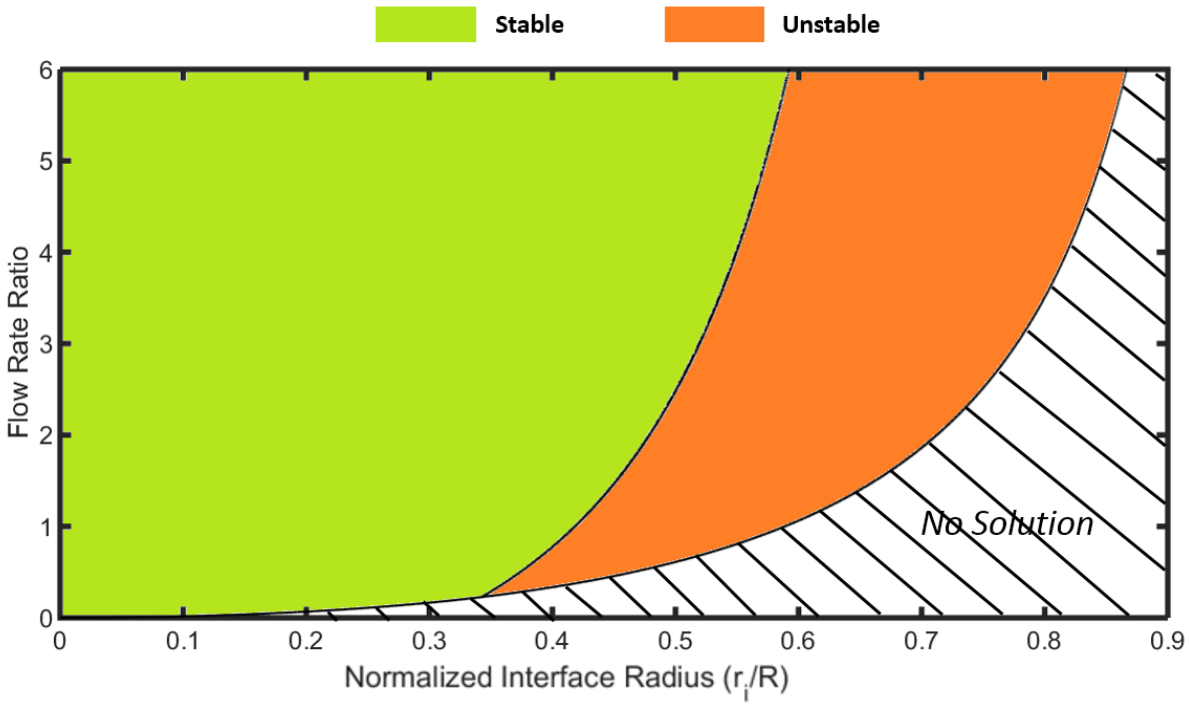

Figure 3-6 plot of flow rate ratio vs. normalized interface radius for $B=2.5$

In Figure 3-6, the green region is stable case where a plug is formed around the core and the red region shows the unstable case where the lubricant is fully yielded. For the static case, the flow rate ratio is always infinity which is not appeared in this figure. The hashed region in Figure 3-6 shows there is no solution.

Chapter 4. Comparison and Discussion

In this chapter. . .

Results obtained from experiments, simulations and analytical model will be presented and comparisons between the results will be given.

4.1. Viscosity ratio vs. interface radius

Figure 4-1 shows the plot of viscosity ratio vs. normalized interface radius for the data obtained from experiments, simulations and analytical solutions. Bingham number in all the experiments are 2.5±0.4. By plotting the two ends of this interval (B=2.1 and B=2.9), they will all show the points are located inside the stable region. For simplicity, the predicted borders are plotted based on the average Bingham number of 2.5.

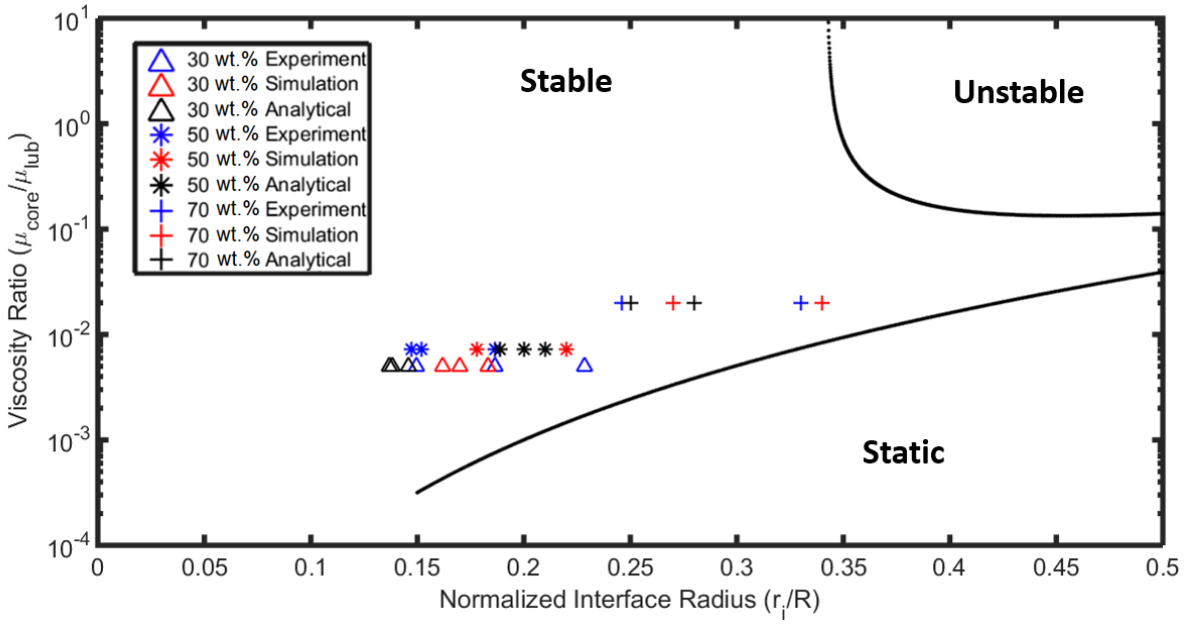

Figure 4-1 Viscosity ratio vs. normalized interface radius, *B=2.5*

According to the data from the experiments and the models, the points are far from the boundaries between stable and unstable cases. Figure 4-2 shows the simulations for higher flow rate ratios and higher viscosity ratios (square and crossed-square shapes). It confirms that the boundary predicted by the analytical model is consistent with the simulation cases. The velocity profiles for a stable and an unstable case are shown in Figure 4-2.

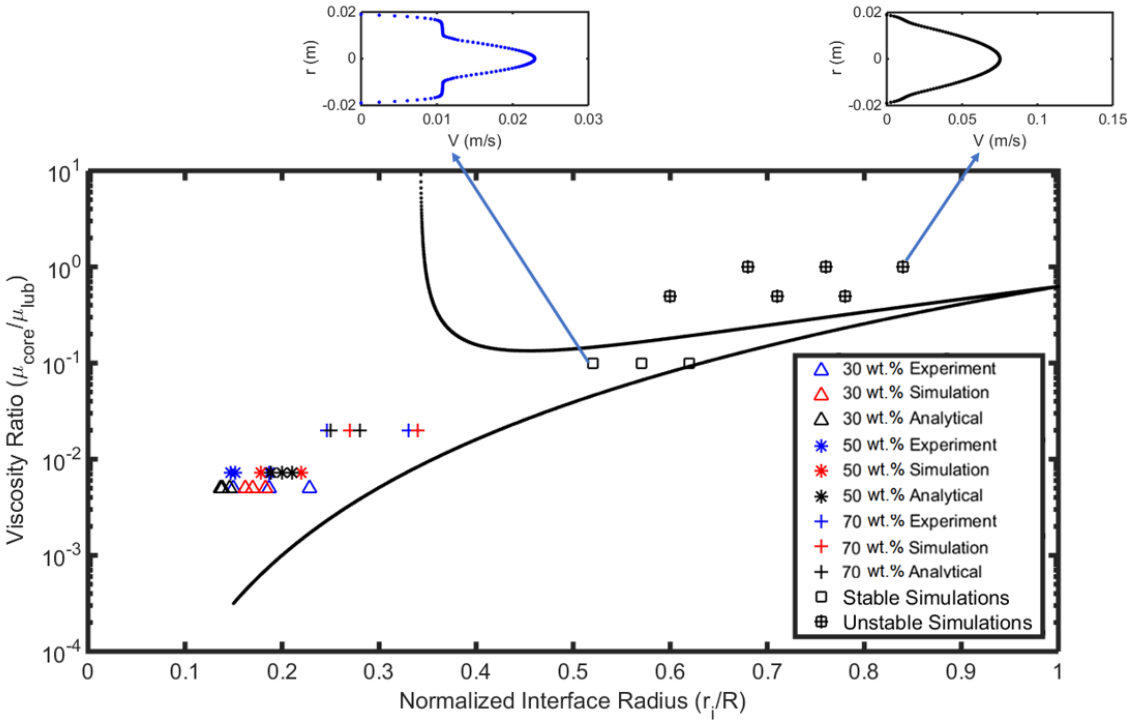

Figure 4-2 Viscosity ratios vs. normalized interface radius for the experiments and the simulations

4.2. Interface radius

Interface radius predicted by the simulation and the analytical model are presented in Figures 4-3 and 4-4 alongside the measured values from the experiments. Ideally, we expect the points lie on the y=x line.

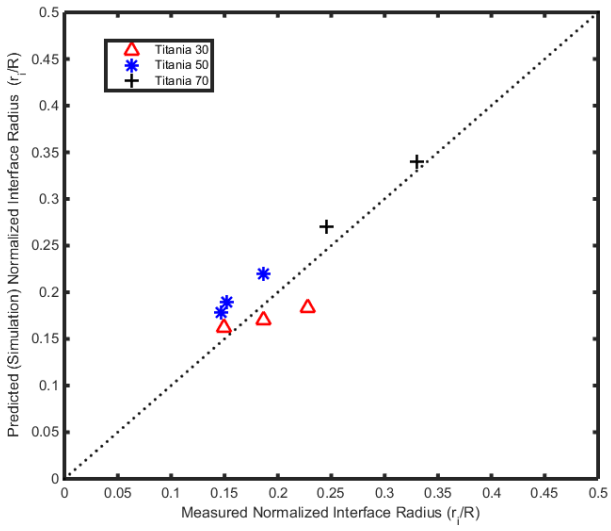

Figure 4-3 Predicted interface (Numerical model) vs. measured interface

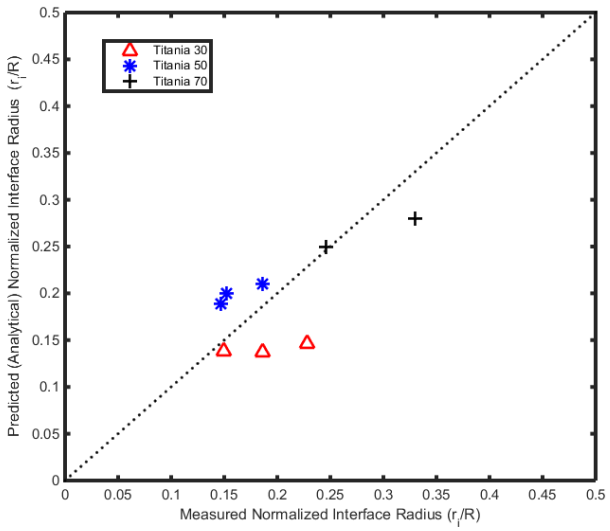

Figure 4-4 Predicted interface (Analytical model) vs. measured interface

The best agreement between experiments and simulation results was observed for the experiments with Titania 70 wt. % which was the ultimate goal of this study. Figure 4-3 shows the two points related to Titania 70 wt. % experiments are almost located on the y=x line.

Figure 4-4 shows the interface radius obtained from the analytical model vs. the measured value from the experiments. In this figure, larger difference was observed between the predicted and measured interface radius. By comparing Figures 4-3 and 4-4, it is concluded that the simulation results are closer to the data obtained from the experiment.

4.3. Flow rate vs. Normalized interface radius

Flow rate ratio vs. normalized interface radius for the data obtained from the experiments, simulation and analytical model are presented in Figure 4-5. The points are showing the experiments with stable annular flow. The curves show the borders between stable and unstable

cases for B=2.5. The static case (where there is no movement of lubricant) happens at the infinity because of flow rate ratio of infinity.

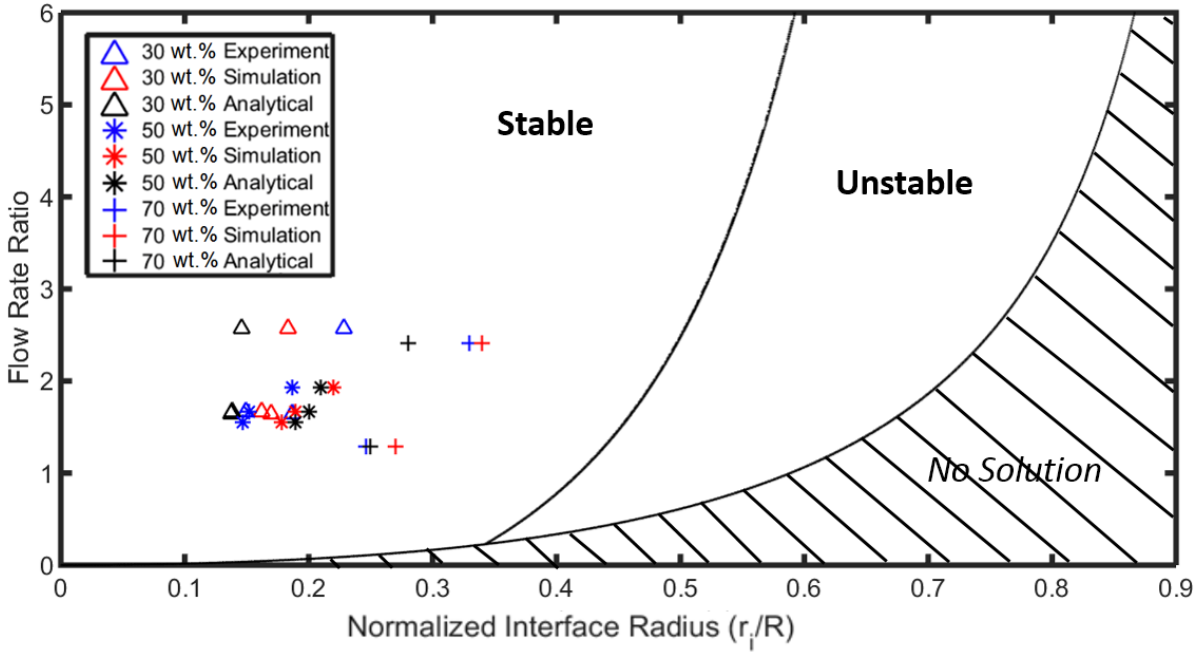

Figure 4-5 Flow rate ratio (core to lub. fluid) vs. normalized interface radius

According to Figure 4-5, the experiment points are located far from the boundary between the stable and the unstable region. It shows the instability is observed when the interface radius is larger. As it is understood from the numerical models and the experiments, increasing the core fluid viscosity while keeping the lubricant rheology unchanged (increasing the viscosity ratio of core to lubricating fluid) tends to increase the interface diameter. Since the unstable case is happening for larger interfaces, it is expected to reach unstable flow by increasing the viscosity of the core fluid at the same flow rate ratio.

Moreover, we can reach the unstable region by reducing the yield stress property of the lubricant. In other words, if diluter Carbomer gel is used as the lubricant, we would expect the boundary between the stable and unstable regions move towards left. That indicates the flow becomes

unstable for smaller interface radius. Additionally, reducing yield stress of the lubricant means the unyielded plug around the core fluid in the stable case can be more easily broken and the result will be the unstable flow. The hashed region in Figure 4-5 shows the area where there is no solution.

Now, by plotting the extrapolated data obtained from the simulations, we will have Figure 4-6 which shows flow rate ratio of core fluid to lubricating fluid vs. the normalized interface radius. The stable points (square shape) are located in stable region and the unstable points (crossed-square shape) are locate in unstable region which is predicted well by the analytical model.

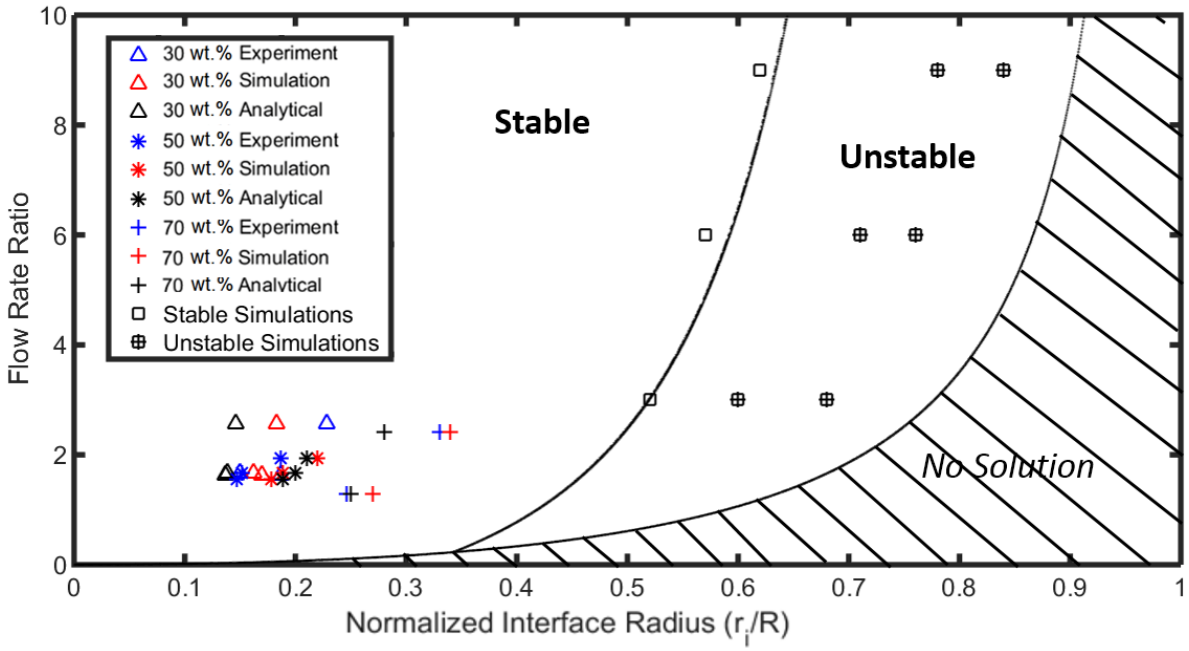

Figure 4-6 Plot of flow rate ratio vs. normalized interface radius with extrapolated data from simulation

4.4. Measurement Errors

In Figures 4-3 and 4-4, results of the experimental, numerical and analytical studies are brought together. They show most of the predicted radii are within ±15% of the measured values. This error is probably caused by the following factors:

4.4.1. Rheology of the two fluids

In order to predict the interface radius with analytical solution, Rheology data for the core fluids and lubricating fluid should be measured precisely for the proper range of shear rates in the experiments. The viscosity models are sensitive to the range of the shear rates and this range should be the range which experiment is performing [8].

Moreover, Bingham model is used for the rheology of the yield stress fluid (Carbomer gel). There is an overestimation of yield stress by using Bingham model that is shown in Figure 4-7.

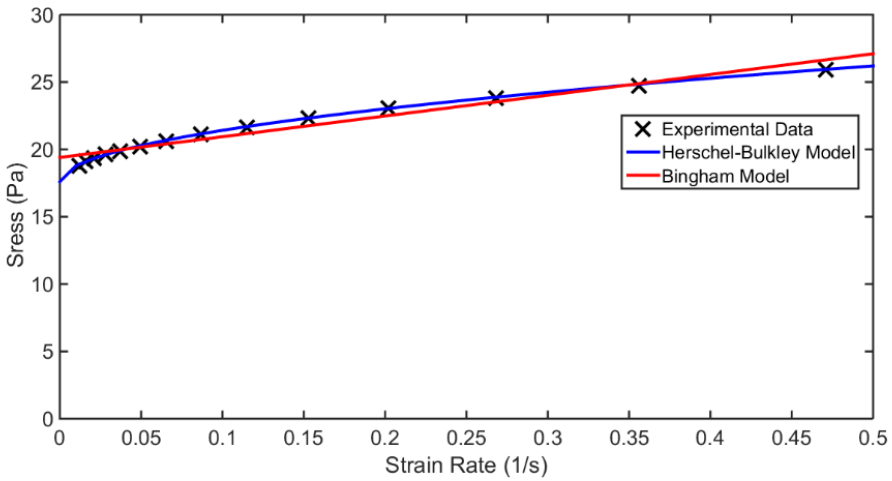

Figure 4-7 Flow curve of Carbomer 0.2 wt.%

4.4.2. Flow rates of the fluids

The flow rates that were measured in the experiments are used as the inputs of the simulation and analytical models. The uncertainty in the measurement of the flow rates which is computed by dividing the mass of the fluids by the time may result in some errors in the predicted interface radius by the simulation and analytical models. The introduced error in flow rater measurement is estimated to be ± 0.25 mL/s.

4.4.3. Different densities

Analytical model is derived for two iso-density fluids. However, in our case, the density of the fluids is not the same and this could be a reason why the model and experiment are not perfectly matched.

Chapter 5. Conclusion and Future Directions

In this chapter. . .

The conclusion of this study will be presented. Additionally, the possible directions for the future of this work will be proposed.

This study shows that the core-annular flow of a suspension lubricated by a yield stress fluid can be established which eliminates the contact of the suspension and the tube wall as the main goal. Moreover, the effect of increasing the concentration of Titania suspension, previously defined as a desirable factor in speeding up the SPS process, is investigated and this work demonstrates the possibility of establishing a stable, multi-layer flow with high suspension concentration and high density ratio (of core fluid to lubricating fluid).

One of the goals in this study was to reduce the thickness of the lubricating fluid to make the transportation of the suspensions more efficient. The experiments and numerical simulations suggest increasing the viscosity of the core fluid (as a result of increasing the solid content concentration in the suspensions) can lead to a larger interface diameter and thinner lubricating layer. Additionally, from analytical solutions, higher flow rate ratio of core fluid to lubricating fluid will increase the interface radius. By increasing both (viscosity ratio and flow rate ratio), we are approaching the unstable region. Briefly, the results showed us:

- Interface radius increased with the flow rate ratio of the core to lubricating fluid.
- Increasing the concentrations of Titania suspensions resulted in higher viscosity ratio of core to lubricating fluid which leads to larger interface radius.
- The interface becomes smoother by increasing the concentration of Titania suspensions.
- The highest density ratio of core fluid to lubricating fluid that was achieved in this study was 2.2 which was greater than the previous studies in this field [10].

5.1. Future directions

Here are some suggestions for the future development of this study that can shed more light on the visco-plastic lubrication and the limitations in the transportation processes.

- Investigating the flow for smaller yield stress

  By reducing the concentration of Carbomer gel, stable annular flow still can be established. Reducing the concentration results in higher viscosity ratio of core to lubricating fluid (by keeping the core fluid constant) which means approaching to the unstable case. However, using less viscous lubricant can facilitate the transportation and reduce the amount of Carbomer powder that is used which is desirable.

- Study the effect of different core fluids

  In this study, Titania suspensions were used as the core fluid. Replacing Titania with other powders or even changing the core fluid can be helpful to investigate the effects of viscosity and density ratios on the flow.

- Using unstable suspensions

  Utilising powders that do not make stable suspensions as the core fluid can be an interesting topic to investigate. Since the suspension is not stable, there will be sedimentation on the interface of the two fluids. Based on the result of this study, It is predicted that these agglomerates will not block the flow and the flow can continue without clogging.

- Investigating different domain geometries

This type of flow can be studied by establishing the annular flow in a tube that is bent for representing the flow in an actual tube where there might be turnings, e.g. a semi circle tube could be an interesting geometry to study the development of core-annular flow.

- Changing the dimensions

  Multilayer flow in smaller dimensions e.g. tube smaller diameters can be studied. For the small scales, it doesn't require large quantities of the fluids. However, it might be challenging to perform experiments at those dimensions.

References

[1] N. Sharifi, M. Pugh, C. Moreau, and A. Dolatabadi, "Developing hydrophobic and superhydrophobic TiO2 coatings by plasma spraying," *Surf. Coatings Technol.*, vol. 289, pp. 29–36, 2016.

[2] N. Sharifi, F. Ben Ettouil, C. Moreau, A. Dolatabadi, and M. Pugh, "Engineering surface texture and hierarchical morphology of suspension plasma sprayed TiO2 coatings to control wetting behavior and superhydrophobic properties," *Surf. Coatings Technol.*, vol. 329, pp. 139–148, 2017.

[3] M. B. Dusseault and others, "Comparing Venezuelan and Canadian heavy oil and tar sands," in *Canadian international petroleum conference*, 2001.

[4] R. Martinez-Palou *et al.*, "Transportation of heavy and extra-heavy crude oil by pipeline: A review," *J. Pet. Sci. Eng.*, vol. 75, no. 3–4, pp. 274–282, 2011.

[5] N. H. Abdurahman, Y. M. Rosli, N. H. Azhari, and B. A. Hayder, "Pipeline transportation of viscous crudes as concentrated oil-in-water emulsions," *J. Pet. Sci. Eng.*, vol. 90, pp. 139–144, 2012.

[6] S. Ghosh, T. K. Mandal, G. Das, and P. K. Das, "Review of oil water core annular flow," *Renew. Sustain. Energy Rev.*, vol. 13, no. 8, pp. 1957–1965, 2009.

[7] I. A. Frigaard, "Super-stable parallel flows of multiple visco-plastic fluids," *J. Nonnewton. Fluid Mech.*, vol. 100, no. 1–3, pp. 49–75, 2001.

[8] C. K. Huen, I. A. Frigaard, and D. M. Martinez, "Experimental studies of multi-layer flows using a visco-plastic lubricant," *J. Nonnewton. Fluid Mech.*, vol. 142, no. 1–3, pp. 150–161, 2007.

[9] E. Mitsoulis, “Flows of viscoplastic materials: models and computations,” *Rheol. Rev.*, vol. 2007, pp. 135–178, 2007.

[10] S. Hormozi, D. M. Martinez, and I. A. Frigaard, “Stable core-annular flows of viscoelastic fluids using the visco-plastic lubrication technique,” *J. Nonnewton. Fluid Mech.*, vol. 166, no. 23–24, pp. 1356–1368, 2011.

[11] S. Hormozi, K. Wielage-Burchard, and I. A. Frigaard, “Entry, start up and stability effects in visco-plastically lubricated pipe flows,” *J. Fluid Mech.*, vol. 673, pp. 432–467, 2011.

[12] D. D. Joseph, R. Bai, K. P. Chen, and Y. Y. Renardy, “Core-annular flows,” *Annu. Rev. Fluid Mech.*, vol. 29, no. 1, pp. 65–90, 1997.

[13] M. A. Moyers-Gonzalez, I. A. Frigaard, and C. Nouar, “Nonlinear stability of a visco-plastically lubricated viscous shear flow,” *J. Fluid Mech.*, vol. 506, pp. 117–146, 2004.

[14] P. Coussot, “Yield stress fluid flows: A review of experimental data,” *J. Nonnewton. Fluid Mech.*, vol. 211, pp. 31–49, 2014.

[15] X. Huang and M. H. Garcia, “A Herschel--Bulkley model for mud flow down a slope,” *J. Fluid Mech.*, vol. 374, pp. 305–333, 1998.

[16] P. Saramito, “A new elastoviscoplastic model based on the Herschel--Bulkley viscoplastic model,” *J. Nonnewton. Fluid Mech.*, vol. 158, no. 1–3, pp. 154–161, 2009.

[17] F. De Larrard, C. F. Ferraris, and T. Sedran, “Fresh concrete: a Herschel-Bulkley material,” *Mater. Struct.*, vol. 31, no. 7, pp. 494–498, 1998.

[18] “ANSYS Fluent (2011). Fluent 14 documentation. User’s guide.”

Appendix

Carbopol preparation procedure

Recipe for preparing 2L of Carbomer gel (0.2 wt.%)

- Filling a beaker with 2L of distilled water
- Putting the beaker on a magnetic mixer and setting the rotation speed to 900 rpm
- Adding 4g of Carbomer powder to the beaker
- Mixing at 900 rpm for 2 hours until complete dissolving
- Adding solution of NaOH (1.5 M) to reach pH=6.4

Titania suspension preparation procedure

Recipe for preparing 1L of Titania 30 wt.% suspension

- Filling a beaker with 700 mL of distilled water
- Putting the beaker on a magnetic mixer and setting the rotation speed to 900 rpm
- Turning on the sonicator and fixing the power on 50 W
- Adding Titania powder to the water by spatula
- Increasing the power of sonication by 5 W after adding 100 gr of Titania power
- After adding 300 gr of the Titania powders, set the sonicator at power 40 W and let the solution to agitate for 15 minutes